R. Masson
University Nice Sophia Antipolis, and team COFFEE, INRIA Sophia Antipolis Méditerranée, France
Tel.: +33 (0)4 92 07 62 32
roland.masson@unice.fr

L. Trenty
ANDRA, 1 rue Jean Monnet, 92290 Chatenay-Malabry
Tel.: +33 (0)1 46 11 81 46
laurent.trenty@andra.fr

Y. Zhang
University Nice Sophia Antipolis, and team COFFEE, INRIA Sophia Antipolis Méditerranée, France
Tel.: +33 (0)4 92 07 69 96
yumeng.zhang@unice.fr

Abstract

In this article, three formulations of two phase compositional Darcy flows taking into account phase transitions are compared. The first formulation is the so called natural variable formulation commonly used in reservoir simulation, the second has been introduced in [14] and uses the phase pressures, saturations and component fugacities as main unknowns, and the third is an extension to general compositional two phase flows of the pressure pressure formulation introduced in [2] in the case of two components. The three formulations are shown to lead to equivalent definitions of the phase transitions for our gas liquid thermodynamical model. Then, they are compared numerically in terms of solution and convergence of the Newton type non linear solver on several 1D and 3D test cases including gas appearance and liquid disappearance. The 3D discretization is based on the Vertex Approximate Gradient (VAG) scheme [10] and takes into account discontinuous capillary pressures.

Key words : Darcy flow, two-phase flow, phase transitions, compositional models, finite volume scheme, discontinuous capillary pressures

1 Introduction

The simulation of two phase gas liquid compositional Darcy flows is used in many applications such as the storage of carbon dioxide in saline aquifers, the gas recovery in petroleum reservoirs, the storage of gas in geological reservoirs, or also the safety assessment of geological radioactive waste disposals.

The numerical simulation of such models relies on a proper formulation coupling the mole balance of each component belonging to the set of components $\mathcal{C}$, the pore volume balance, and the hydrodynamical and thermodynamical laws. A major difficulty is to account for the phase transitions induced by the change of phase reactions assumed to be at thermodynamical equilibrium. Many formulations have been proposed in the oil industry (see [8] and the numerous references therein), and more recently for the modelling of liquid gas migration in deep geological formation waste disposal (see for example [3], [2], [5]).

The main objective of this paper is to compare three different formulations for two phase gas (g) liquid (l) compositional Darcy flows taking into account the phase transitions.

The first formulation is the so called natural variable formulation commonly used in the reservoir simulation community and which has been introduced in [6], [7]. It is also known as the switch of variable formulation since it uses a set of unknowns defined by the phase pressures P^l, P^g, the phase saturations S^l, S^g, and the molar fractions of the components $c^\alpha = (c_i^\alpha)_{i\in\mathcal{C}}$ in each phase $\alpha \in Q$ where Q is the set of present phases at each point of the time space domain. The set Q, accounting for the phase transitions, is typically obtained by a negative flash computation [16]. This formulation will be denoted by PSC in the following.

The second formulation has been introduced in [14]. Its main advantage compared with the previous one is to use a fixed set of equations and a fixed set of unknowns defined by the phase pressures P^l, P^g, the phase saturations S^l, S^g, and the component fugacities f_i, $i \in \mathcal{C}$. In this formulation the component molar fractions c^α are expressed as functions of the component fugacities f and of the phase pressures. It results that the component molar fractions of an absent phase are naturally extended by the ones at equilibrium with the present phase leading to a fix set of unknowns and equations. Another advantage is that the phase transitions simply take the form of complementary constraints which avoids negative flash calculations. This formulation will be denoted by PSF in the following.

The last formulation is an extension to general compositional two phase flow of the pressure pressure formulation introduced in [2] in the case of two components. This extension is based on the use of fugacities in addition to the phase pressures in the spirit of [14]. In this formulation, thanks to the extension of the phase pressure P^α in the absence of the phase by $\widetilde{P}^\alpha$ for $\alpha = l, g$, and to the extension of the capillary function $P_c(S^l)$ by its monotone graph, the phase transitions reduce to $S^l = (P_c)^{-1}(\widetilde{P}^g - \widetilde{P}^l)$ and no longer involve inequality constraints. This formulation will be denoted by PPF in the following.

In the subsequent section, the three formulations are detailed and their equivalence is shown to hold under some assumptions on the fugacities. Advantages and drawback of each formulation are also further discussed.

Then, in the numerical test section, the three formulations are compared in terms of non linear convergence on several 1D and 3D test cases with families of refined meshes. The 3D spatial discretization is based on the Vertex Approximate Gradient (VAG) scheme which has been introduced in [10] for diffusion problems in heterogeneous anisotropic media. The VAG scheme has been extended to multiphase Darcy flows in [11] and in [12] in order to take into account discontinuous capillary pressures at the interfaces between different rocktypes using a pressure pressure formulation. It is basically a nodal discretization with an improved treatment of the heterogeneities of the media and of the hydrodynamic laws compared with usual Control Volume Finite Element methods for multiphase Darcy flows [13].

The first test case is a Couplex benchmark proposed by Andra [17], [5] simulating the drying by liquid suction of the geological barrier at the interface with the ventilation gallery. It will be simulated both in 1D and in 3D taking into account two rocktypes and the anisotropy of the media. The second test case is a 1D test case which simulates the drying of a porous media saturated with the liquid phase by gas injection which can arise for instance in the nearwell region of carbon dioxide storage. The third test case simulates the migration of gas in a 3D basin with two capillary barriers in order to compare the compositional formulations with highly contrasted capillary pressures.

2 Formulations of compositional two-phase liquid gas Darcy flows

Let $\mathcal{P} = \{l, g\}$ denote the set of liquid and gas phases assumed to be both defined by a mixture of components $i \in \mathcal{C}$ among which the water component denoted by e which can vaporize in the gas phase, and a set of gaseous components $j \in \mathcal{C} \setminus \{e\}$ which can dissolve in the liquid phase. The number of components is assumed to be at least 2.

For the sake of simplicity, the model will be assumed to be isothermal with a fixed temperature T, and consequently the dependence of the physical laws on the temperature will not always be specified in the following. We will denote by $c^\alpha = \left(c_i^\alpha, i \in \mathcal{C}\right)$ the vector of molar fractions of the components in the phase $\alpha \in \mathcal{P}$ with $\sum_{i\in\mathcal{C}} c_i^\alpha = 1$, and by P^g and P^l the two phase pressures. The mass densities of the phases are denoted by $\rho^\alpha(P^\alpha, c^\alpha)$ and the molar densities by $\zeta^\alpha(P^\alpha, c^\alpha)$, $\alpha \in \mathcal{P}$. They are related by

$$\rho^\alpha(P^\alpha, c^\alpha) = \Big(\sum_{i\in\mathcal{C}} c_i^\alpha M_i\Big)\zeta^\alpha(P^\alpha, c^\alpha),$$

where M_i, $i \in \mathcal{C}$ are the molar masses of the components. The viscosities of the phases are denoted by $\mu^\alpha(P^\alpha, c^\alpha)$, $\alpha \in \mathcal{P}$.

The hydrodynamical Darcy laws are characterized by the relative permeability functions $k_r^\alpha(S^\alpha)$, for both phases $\alpha = g, l$, and by the capillary pressure function $P_c(S^l)$, where S^α,$\alpha = l, g$ denote the saturations of the phases with $S^g + S^l = 1$.

Each component $i \in \mathcal{C}$ will be assumed to be at thermodynamical equilibrium between both phases which is characterized by the equality of its fugacities f_i^α,

$\alpha = g, l$ if both phases are present. The fugacities of the components in the gas phase are assumed to be given by Dalton's law for an ideal mixture of perfect gas

$$f_i^g = c_i^g P^g,\ i \in \mathcal{C}.$$

A correction of type $f_i^g = c_i^g P^g \phi(P^g, T)$ for more general gas mixtures could also be readily taken into account. The fugacities of the components in the liquid phase are assumed to be given by Henry's law for the dissolution of the gaseous components in the liquid phase

$$f_j^l = c_j^l H_j(T),\ j \in \mathcal{C} \setminus \{e\},$$

and by Raoult-Kelvin's law for the water component in the liquid phase [9]

$$f_e^l = c_e^l P_{sat}(T) \exp\Big(\frac{-(P^g - P^l)}{\zeta^l(P^l) RT}\Big),$$

where $P_{sat}(T)$ is the vapor pressure of the pure water. It is assumed in the following, in order to prove rigorously the equivalence between the three formulations, that the liquid molar density in f_e^l the depends only on the liquid pressure P^l, and possibly on the temperature T. It will be denoted by $\zeta^l(P^l)$ in the following.

2.1 Natural variable formulation (PSC)

A classical choice coming from the reservoir simulation community [6], [7] is given by the set of unknowns of the hydrodynamical and thermodynamical laws defined by

$$Q, P^l, P^g, S^l, S^g, c^\alpha,\ \alpha \in Q,$$

where the discrete unknown Q denotes the set of present phases taking the following possible values

$$Q = \{l, g\} \text{ or } \{g\} \text{ or } \{l\}.$$

Then, the model accounts for the mole balance of each component $i \in \mathcal{C}$ with phase velocities given by the Darcy laws and a Fickian diffusion of the components in each phase. It is closed by the pore volume balance $S^g + S^l = 1$, the capillary relation between the two phase pressures, and the thermodynamical equilibrium stating the equality of the fugacities of the present phases. We obtain the following system for the set of unknowns $P^l, P^g, S^l, S^g, c^\alpha,\ \alpha \in Q$

$$\left\{\begin{array}{l} \phi \partial_t \displaystyle\sum_{\alpha \in Q} \zeta^\alpha S^\alpha c_i^\alpha + \mathrm{div}\Big(\sum_{\alpha \in Q} \zeta^\alpha c_i^\alpha \mathbf{V}^\alpha - \phi S^\alpha \zeta^\alpha D_i^\alpha \nabla c_i^\alpha\Big) = 0,\ i \in \mathcal{C}, \\ P^g - P^l = P_c(S^l), \\ \displaystyle\sum_{\alpha \in Q} S^\alpha = 1, \\ S^\alpha = 0,\ \alpha \notin Q, \\ \displaystyle\sum_{i \in \mathcal{C}} c_i^\alpha = 1, \alpha \in Q, \\ f_i^l\Big(c^l, P^g, P^l\Big) = f_i^g\Big(c^g, P^g, P^l\Big),\ i \in \mathcal{C} \text{ if } Q = \{l, g\}, \end{array}\right. \tag{1}$$

together with the Darcy laws for the phase velocities

$$\mathbf{V}^\alpha = -\frac{k_r^\alpha(S^\alpha)}{\mu^\alpha} K\Big(\nabla P^\alpha - \rho^\alpha \mathbf{g}\Big),\ \alpha \in Q.$$

The system (1) must be closed by an equation for the set of present phases Q which is usually obtained by a negative flash computation [16] at fixed phase pressures P^l, P^g and fixed component total molar fractions

$$z_i = \frac{\sum_{\alpha\in Q} \zeta^\alpha S^\alpha c_i^\alpha}{\sum_{\alpha\in Q} \zeta^\alpha S^\alpha},\ i \in \mathcal{C}.$$

The negative flash computes the gas phase molar fraction $\theta^g \in \mathbb{R}$, possibly negative, and the gas and liquid component molar fractions $\bar{c}^g$ and $\bar{c}^l$ at equilibrium such that

$$\left\{\begin{array}{l} z_i = \theta^g \bar{c}_i^g + (1-\theta^g)\bar{c}_i^l,\ i \in \mathcal{C}, \\ \displaystyle\sum_{i\in\mathcal{C}} \bar{c}_i^\alpha = 1,\ \alpha \in \mathcal{P}, \\ f_i^l\Big(\bar{c}^l, P^g, P^l\Big) = f_i^g\Big(\bar{c}^g, P^g, P^l\Big),\ i \in \mathcal{C}, \\ \bar{c}_i^g \geq 0,\ \bar{c}_i^l \geq 0,\ i \in \mathcal{C}. \end{array}\right. \tag{2}$$

Then, the set of present phases Q is defined by

$$\left\{\begin{array}{c} Q = \{l,g\} \text{ and } \theta^g \in]0,1[, \\ \text{or} \\ Q = \{l\} \text{ and } \theta^g \leq 0, \\ \text{or} \\ Q = \{g\} \text{ and } \theta^g \geq 1. \end{array}\right. \tag{3}$$

In other words, the negative flash computes the solution $\bar{c}^g$, $\bar{c}^l$, θ^g satisfying the thermodynamical equilibrium and the component total mole balance, and the signs of the phase molar fractions θ^g and $\theta^l = 1-\theta^g$ provide the criteria for the phase appearance or disappearance.

Let us give below a simpler definition of the set Q that will be used to show the equivalence of the natural variable formulation with the two other formulations presented in the next two subsections. For $Q = \{l\}$, let us define the component molar fractions in the gas phase in equilibrium with the component molar fractions in the liquid phase (note that $\tilde{c}^g$ differs in general from $\bar{c}^g$)

$$\left\{\begin{array}{l} \tilde{c}_e^g = c_e^l \frac{P_{sat}(T)}{P_g} \exp\Big(\frac{-(P^g-P^l)}{\zeta^l(P^l)RT}\Big), \\ \tilde{c}_j^g = c_j^l \frac{H_j(T)}{P_g},\ j \in \mathcal{C}\setminus\{e\}, \end{array}\right. \tag{4}$$

and, for $Q = \{g\}$, the component molar fractions in the liquid phase in equilibrium with the component molar fractions in the gas phase (note that $\tilde{c}^l$ differs in general from $\bar{c}^l$)

$$\left\{\begin{array}{l} \tilde{c}_e^l = c_e^g \frac{P^g}{P_{sat}(T)} \exp\Big(\frac{(P^g-P^l)}{\zeta^l(P^l)RT}\Big), \\ \tilde{c}_j^l = c_j^g \frac{P^g}{H_j(T)},\ j \in \mathcal{C}\setminus\{e\}. \end{array}\right. \tag{5}$$

Then, the coupled system (1)-(3) is equivalent to the system (1) coupled with the following simpler conditions on the set of present phases Q:

$$\begin{cases} Q = \{l, g\} \text{ and } S^g > 0, S^l > 0, \\ \qquad \text{or} \\ Q = \{l\} \text{ and } \sum_{i \in \mathcal{C}} \tilde{c}_i^g \leq 1, \\ \qquad \text{or} \\ Q = \{g\} \text{ and } \sum_{i \in \mathcal{C}} \tilde{c}_i^l \leq 1. \end{cases} \tag{6}$$

Proof: Thanks to our assumptions on the fugacities, the negative flash reduces to the following Rachford Rice equation for the molar fraction of the gas phase θ^g (see [16])

$$f^{rc}(\theta^g) = \sum_{i \in \mathcal{C}} (\bar{c}_i^g - \bar{c}_i^l) = \sum_{i \in \mathcal{C}} \frac{(K_i - 1) z_i}{1 + \theta^g (K_i - 1)} = 0,$$

with coefficients $K_j = \frac{H_j(T)}{P^g}$ for $j \in \mathcal{C} \setminus \{e\}$ and $K_e = \frac{P_{sat}(T)}{P^g} \exp\Big(\frac{-(P^g - P^l)}{\zeta^l(P^l) RT}\Big)$ depending only on P^l, P^g and T.

Let us define $\bar{\mathcal{C}} = \{i \in \mathcal{C} \,|\, z_i \neq 0, K_i \neq 1\}$. If $\bar{\mathcal{C}} = \emptyset$, this is a degenerate case for which both phases cannot be distinguished and hence can be considered as present for both formulations. If $\bar{\mathcal{C}} \neq \emptyset$, let us define $K_{max} = \max_{i \in \bar{\mathcal{C}}} K_i$, $K_{min} = \min_{i \in \bar{\mathcal{C}}} K_i$, $\theta_0 = \frac{1}{1 - K_{max}}$ and $\theta_1 = \frac{1}{1 - K_{min}}$. To fix ideas, we will consider the case $\theta_0 < 0$ and $\theta_1 > 1$, the extension to the two other cases $\theta_0 \geq \theta_1 > 1$, or $\theta_1 \leq \theta_0 < 0$ is not difficult. It results that the Rachford Rice function f^{rc} is strictly decreasing and admits a unique solution θ^g such that $\bar{c}_i^\alpha \geq 0$, $i \in \mathcal{C}$, $\alpha \in \mathcal{P}$ on the interval $]\theta_0, \theta_1[$.

In order to prove the equivalence of the system (3)-(1) with the system (6)-(1), let us consider the three cases $Q = \{l, g\}$, $Q = \{l\}$, $Q = \{g\}$. First if $Q = \{l, g\}$, then according to the system (1), the equilibrium equations are already satisfied which means that $c^\alpha = \bar{c}^\alpha$ for $\alpha = l, g$ and

$$\theta^g = \frac{\zeta^g S^g}{\sum_{\alpha = l,g} \zeta^\alpha S^\alpha}.$$

It is then clear (assuming a positive total number of moles) that the condition $\theta^g > 0$ and $\theta^l = 1 - \theta^g > 0$ in (3) is equivalent to $S^g > 0$ and $S^l > 0$ in (6).

Next for $Q = \{l\}$, let us prove that the gas appearance criteria $\theta^g > 0$ in (3) is equivalent to the gas appearance criteria $\sum_{i \in \mathcal{C}} \tilde{c}_i^g > 1$ in (6). In such a case $z_i = c_i^l$ which implies that $f^{rc}(0) = \sum_{i \in \mathcal{C}} \tilde{c}_i^g - 1$. Using the monotonicity of f^{rc} and $0 \in]\theta_0, \theta_1[$, it results that the gas appearance criteria $\theta^g > 0$ is equivalent to $0 = f^{rc}(\theta^g) < f^{rc}(0) = \sum_{i \in \mathcal{C}} \tilde{c}_i^g - 1$. The proof of equivalence for the case $Q = \{g\}$ is similar to the case $Q = \{l\}$.

The system (1)-(6)-(4)-(5) is discretized using a fully implicit Euler integration in time and a finite volume discretization in space (see subsection 3.3 for the detailed example of the Vertex Approximate Gradient discretization). The mobility terms

are upwinded with respect to the sign of the phase Darcy flux, and an harmonic averaging is chosen for the Fick flux terms $\phi S^\alpha \zeta^\alpha$ (see [1],[6],[7]).

The non linear system arising from this discretization is solved at each time step by a Newton Raphson algorithm coupled with a fixed point update of the set of present phases Q in each cell using (6)-(4)-(5). In order to reduce the size of the linear system to $\#\mathcal{C}$ equations and unknowns in each cell, the set of unknowns is splitted into $\#\mathcal{C}$ primary unknowns and remaining secondary unknowns. This splitting is done cell by cell depending on the set of present phases in the cell in such a way that the Schur complement is well defined (see [6],[7],[11]). For our thermodynamical system, to fix ideas let j_1 denote the component with the largest Henry constant H_{j_1}, then our set of primary unknowns is defined by

$$\left\{ \begin{array}{ll} P^g, S^l, c_i^g, i \in \mathcal{C} \setminus \{j_1, e\} & \text{for } Q = \{l, g\}, \\ P^g, c_i^l, i \in \mathcal{C} \setminus \{e\} & \text{for } Q = \{l\}, \\ P^g, c_i^g, i \in \mathcal{C} \setminus \{e\} & \text{for } Q = \{g\}, \end{array} \right. \tag{7}$$

which garantees the invertibility of the closure laws w.r.t. the secondary unknowns provided that $H_{j_1} \neq P_{sat}(T)\exp\Big(\frac{-(P^g - P^l)}{\zeta^l(P^l)RT}\Big)$ (for $Q = \{l, g\}$) which should not physically arise.

The main advantage of this formulation is to use the natural set of unknowns for the hydrodynamical and thermodynamical laws and to extend to a large class of compositional Darcy flow models ranging from immiscibility to full miscibility (see [11]). On the other hand, its main drawbacks are an additional complexity to deal with sets of unknowns and equations depending on the set Q, and the use of a fixed point algorithm to compute the set of present phases Q at each point of the space time domain. The efficiency of this formulation has mainly been shown for reservoir simulation test cases with complex thermodynamics, two and tri phase Darcy flows, but with usually small capillary effects and the use of a reference pressure in the thermodynamical state laws rather than the phase pressures. In the next section it will be assessed and compared with the two other formulations on test cases with both strong or weak capillary effects.

2.2 Pressures, saturations and fugacities formulation (PSF)

We recall in this subsection the formulation introduced in [14] using a fix set of unknowns defined by the phase pressures P^l, P^g, the phase saturations S^l, S^g, and the component fugacities $f = \Big(f_i, i \in \mathcal{C}\Big)$. The component molar fractions c^α of each phase $\alpha = l, g$ are assumed to be defined as the unique solution denoted by $\widetilde{c}^\alpha\Big(f, P^g, P^l\Big)$ of the system

$$f_i^\alpha\Big(c^\alpha, P^g, P^l\Big) = f_i,\ i \in \mathcal{C}. \tag{8}$$

If the phase α is present, ie $S^\alpha > 0$, the function $\widetilde{c}^\alpha\Big(f, P^g, P^l\Big)$ will match with the component molar fractions c^α. If the phase is absent, the function $\widetilde{c}^\alpha\Big(f, P^g, P^l\Big)$ will match with the extension of the component molar fractions by those in equilibrium

with the component molar fractions in the present phase as in (4) and (5). This extension is clearly arbitrary for the conservation equations since the component molar fractions are always in factor of the saturation or the relative permeability of the phase both vanishing for an absent phase. On the other hand, the choice of this extension will affect the convergence of the non linear solver to the solution. In our case, thanks to our assumptions on the fugacities, we simply have the following expressions of the extended component molar fractions:

$$\left\{\begin{array}{l} \widetilde{c}_e^l\Big(f,P^g,P^l\Big) = \frac{f_e}{P_{sat}(T)}\exp\Big(\frac{(P^g-P^l)}{\zeta^l(P^l)RT}\Big), \\ \widetilde{c}_j^l\Big(f,P^g,P^l\Big) = \frac{f_j}{H_j(T)},\ j\in\mathcal{C}\setminus\{e\}, \\ \widetilde{c}_e^g\Big(f,P^g,P^l\Big) = \frac{f_e}{P^g}, \\ \widetilde{c}_j^g\Big(f,P^g,P^l\Big) = \frac{f_j}{P^g},\ j\in\mathcal{C}\setminus\{e\}. \end{array}\right. \tag{9}$$

Note that the PSF formulation can be defined for more general fugacity models provided that the equations $f = f^\alpha(c^\alpha, P^g, P^l)$ can be inverted for both phases $\alpha\in\mathcal{P}$. Finally, the set of equations obtained in [14] for the set of unknowns P^l, P^g, S^l, S^g, f is defined by

$$\left\{\begin{array}{l} \phi\partial_t\sum\limits_{\alpha\in\mathcal{P}}\zeta^\alpha S^\alpha\widetilde{c}_i^\alpha + \mathrm{div}\Big(\sum\limits_{\alpha\in\mathcal{P}}\zeta^\alpha\widetilde{c}_i^\alpha\mathbf{V}^\alpha - \phi S^\alpha\zeta^\alpha D_i^\alpha\nabla\widetilde{c}_i^\alpha\Big) = 0,\ i\in\mathcal{C}, \\ S^g + S^l = 1, \\ P^g - P^l = P_c(S^l), \\ \Big(1-\sum\limits_{i\in\mathcal{C}}\widetilde{c}_i^l\Big)S^l = 0,\ 1-\sum\limits_{i\in\mathcal{C}}\widetilde{c}_i^l\geq 0,\ S^l\geq 0, \\ \Big(1-\sum\limits_{i\in\mathcal{C}}\widetilde{c}_i^g\Big)S^g = 0,\ 1-\sum\limits_{i\in\mathcal{C}}\widetilde{c}_i^g\geq 0,\ S^g\geq 0, \end{array}\right. \tag{10}$$

with the Darcy phase velocities

$$\mathbf{V}^\alpha = -\frac{k_r^\alpha(S^\alpha)}{\mu^\alpha}K\Big(\nabla P^\alpha - \rho^\alpha\mathbf{g}\Big),\ \alpha\in\mathcal{P}.$$

Its equivalence with the previous formulation is readily obtained in view of (4), (5) and (6), and setting $c^\alpha = \widetilde{c}^\alpha$ if $S^\alpha > 0$, $\alpha\in\mathcal{P}$.

The space and time discretization is the same as for the previous formulation, and the non linear system arising at each time step is solved by a semi-smooth Newton algorithm (Newton-Min) adapted to complementary constraints (see [15], [4]). This is one advantage of this formulation to fit into the semi-smooth Newton framework. The other advantage is to lead to a fix set of unknowns and equations. Nevertheless, the choice of the secondary unknowns to be eliminated from the linearized system using the closure laws is also as above dependent on the set of present phases. For our thermodynamical system, as for the PSC formulation, let j_1 denote the component with the largest Henry constant H_{j_1}, then our set of primary unknowns is defined by

$$\left\{\begin{array}{ll} P^g, S^l, f_i, i\in\mathcal{C}\setminus\{j_1,e\} & \text{if } S^l>0 \text{ and } S^g>0, \\ P^g, f_i, i\in\mathcal{C}\setminus\{e\} & \text{if } S^l=0 \text{ or } S^g=0, \end{array}\right. \tag{11}$$

which again garantees the invertibility of the closure laws w.r.t. the secondary unknowns provided that $H_{j_1} \neq P_{sat}(T)\exp\Big(\frac{-(P^g-P^l)}{\zeta^l(P^l)RT}\Big)$.

The next formulation goes a step further since it eliminates all the inequality constraints, and leads to a fix choice of the secondary unknowns in the linear systems.

2.3 Pressures, and fugacities formulation (PPF)

The aim of the following formulation is to avoid any inequalities in the set of equations while taking into account phase transitions. This has been achieved in [2] for a liquid gas two components model taking into account the dissolution of the gaseous components in the liquid phase. We propose below an extension of this formulation to compositional two phase flows with an arbitrary number of components.

The starting point is the formulation (10) of the previous section based on the definition of the extended component molar fractions $\widetilde{c}^\alpha\Big(f, P^g, P^l\Big),\ \alpha = l, g$ (9). The next step is to extend the definition of the phase pressures denoted by $\widetilde{P}^\alpha$ in the absence of the phase writing that

$$\sum_{i\in\mathcal{C}} \widetilde{c}_i^\alpha(f, \widetilde{P}^g, \widetilde{P}^l) = 1,\ \alpha \in \mathcal{P}.$$

This definition clearly matches with the phase pressure P^α if the phase α is present and defines an extension of the phase pressure if the phase is absent.

To deal with phase appearance and disappearance, one extends the graph of the capillary pressure curve by its monotone graph ie by $S^l = 1,\ P_c \in [P_c(1), -\infty[$ to deal with the single phase liquid - two phase gas liquid transition, and by $S^l = 0$, $P_c \in [P_c(0), +\infty[$ to deal with the single phase gas - two phase gas liquid transition. We will denote by $\widetilde{P}_c$ the resulting monotone graph and its inverse by $\widetilde{P}_c^{-1}$. Then, the equation

$$S^l = \widetilde{P}_c^{-1}(\widetilde{P}^g - \widetilde{P}^l), \tag{12}$$

together with the definition of the extended pressures suffice to account for the phase transitions. More specifically, we will show that the system

$$\left\{\begin{array}{r} S^g + S^l = 1, \\ P^g - P^l = P_c(S^l), \\ \Big(\sum_{i\in\mathcal{C}} \widetilde{c}_i^\alpha(f, P^g, P^l) - 1\Big) S^\alpha = 0,\ \alpha = l, g, \\ \sum_{i\in\mathcal{C}} \widetilde{c}_i^\alpha(f, P^g, P^l) \leq 1,\ \alpha = l, g, \\ S^\alpha \geq 0,\ \alpha = l, g, \end{array}\right. \tag{13}$$

and the system

$$\left\{\begin{array}{r} S^g + S^l = 1, \\ S^l = \widetilde{P}_c^{-1}(\widetilde{P}^g - \widetilde{P}^l), \\ \sum_{i\in\mathcal{C}} \widetilde{c}_i^\alpha(\widetilde{f}, \widetilde{P}^g, \widetilde{P}^l) = 1,\ \alpha = l, g, \end{array}\right. \tag{14}$$

lead to equivalent conditions on the physical unknowns defined by both saturations S^g, S^l, the pressures $P^\alpha = \widetilde{P}^\alpha$ and the molar fractions $c^\alpha = \widetilde{c}^\alpha(\widetilde{f}, \widetilde{P}^g, \widetilde{P}^l) = \widetilde{c}^\alpha(f, P^g, P^l)$ for the present phases $\alpha = l, g$ such that $S^\alpha > 0$. This definition also specifies the correspondance between the component fugacities f and $\widetilde{f}$ in the sense that $f = f^\alpha(c^\alpha, P^g, P^l)$ and $\widetilde{f} = f^\alpha(c^\alpha, \widetilde{P}^g, \widetilde{P}^l)$ for all $\alpha = l, g$ such that $S^\alpha > 0$.

Proof: For both systems, the saturations are such that $S^g + S^l = 1$ and $S^g \geq 0$, $S^l \geq 0$. Hence we will consider the three cases corresponding to (i) $S^l > 0$ and $S^g = 1 - S^l > 0$, to (ii) $S^l = 1$ and $S^g = 0$, and to (iii) $S^l = 0$ and $S^g = 1$.

(i) if both phases are present ie $S^l > 0$ and $S^g = 1 - S^l > 0$, then $P^l = \widetilde{P}^l$, $P^g = \widetilde{P}^g$, $f = \widetilde{f}$, and the equivalence of the conditions on the physical unknowns for both systems is clear.

(ii) If the gas phase is absent ie $S^l = 1$, $S^g = 0$, the physical unknowns are defined by the pressure $P^l = \widetilde{P}^l$, and the liquid molar fractions $c^l = \widetilde{c}^l(\widetilde{f}, \widetilde{P}^g, P^l) = \widetilde{c}^l(f, P^g, P^l)$ such that $\sum_{i\in\mathcal{C}} c_i^l = 1$. In other words, given P^l and c^l such that $\sum_{i\in\mathcal{C}} c_i^l = 1$, we need to prove that the condition on c^l, P^l

$$\sum_{i\in\mathcal{C}} \widetilde{c}_i^g(f, P^g, P^l) \leq 1,$$

with $P^g = P^l + P_c(1)$ and $f = f^l(c^l, P^g, P^l)$, is equivalent to the condition

$$\widetilde{P}_c^{-1}(\widetilde{P}^g - P^l) = 1,$$

with $\widetilde{P}^g$ and $\widetilde{f}$ such that $\sum_{i\in\mathcal{C}} \widetilde{c}_i^g(\widetilde{f}, \widetilde{P}^g, P^l) = 1$, $\widetilde{f} = f^l(c^l, \widetilde{P}^g, P^l)$. The inequality $\sum_{i\in\mathcal{C}} \widetilde{c}_i^g(f, P^g, P^l) \leq 1$ is equivalent to

$$\sum_{i\in\mathcal{C}} \widetilde{c}_i^g(f^l(c^l, P^g, P^l), P^g, P^l) \leq 1 = \sum_{i\in\mathcal{C}} \widetilde{c}_i^g(f^l(c^l, \widetilde{P}^g, P^l), \widetilde{P}^g, P^l).$$

It is easy to check in our case that the function

$$g^{gl}(u) = \sum_{i\in\mathcal{C}} \widetilde{c}_i^g(f^l(c^l, u, P^l), u, P^l)$$

is non increasing. Hence the latter inequality is equivalent to

$$\widetilde{P}^g \leq P^g = P^l + P_c(1),$$

and hence to $1 = \widetilde{P}_c^{-1}(\widetilde{P}^g - P^l)$.

(iii) If the liquid phase is absent ie $S^l = 0$, $S^g = 1$, the physical unknowns are defined by the pressure $P^g = \widetilde{P}^g$, and the gas molar fractions $c^g = \widetilde{c}^g(\widetilde{f}, P^g, \widetilde{P}^l) = \widetilde{c}^g(f, P^g, P^l)$ such that $\sum_{i\in\mathcal{C}} c_i^g = 1$. In other words, given P^g and c^g such that $\sum_{i\in\mathcal{C}} c_i^g = 1$, we need to prove that the condition on c^g, P^g

$$\sum_{i\in\mathcal{C}} \widetilde{c}_i^l(f, P^g, P^l) \leq 1,$$

with $P^l = P^g - P_c(0)$ and $f = f^g(c^g, P^g, P^l)$, is equivalent to the condition

$$\widetilde{P}_c^{-1}(P^g - \widetilde{P}^l) = 0,$$

with $\widetilde{P}^l$ and $\widetilde{f}$ such that $\sum_{i\in\mathcal{C}} \widetilde{c}_i^l(\widetilde{f}, P^g, \widetilde{P}^l) = 1$, $\widetilde{f} = f^g(c^g, P^g, \widetilde{P}^l)$. The inequality $\sum_{i\in\mathcal{C}} \widetilde{c}_i^l(f, P^g, P^l) \leq 1$ is equivalent to

$$\sum_{i\in\mathcal{C}} \widetilde{c}_i^l(f^g(c^g, P^g, P^l), P^g, P^l) \leq 1 = \sum_{i\in\mathcal{C}} \widetilde{c}_i^l(f^g(c^g, P^g, \widetilde{P}^l), P^g, \widetilde{P}^l).$$

It is easy to check in our case that the function

$$g^{lg}(u) = \sum_{i\in\mathcal{C}} \widetilde{c}_i^l(f^g(c^g, P^g, u), P^g, u)$$

is non increasing (the molar density of the liquid phase is non decreasing w.r.t. the liquid pressure). Hence the latter inequality is equivalent to

$$P^g - P_c(0) = P^l \geq \widetilde{P}^l,$$

ie to $0 = \widetilde{P}_c^{-1}(P^g - \widetilde{P}^l)$.

Finally we obtain the following system of equations for the set of unknowns $\widetilde{P}^g, \widetilde{P}^l, f$

$$\left\{\begin{array}{l} \phi\partial_t \sum_{\alpha\in\mathcal{P}} \zeta^\alpha S^\alpha \widetilde{c}_i^\alpha + \mathrm{div}\Big(\sum_{\alpha\in\mathcal{P}} \zeta^\alpha \widetilde{c}_i^\alpha \mathbf{V}^\alpha - \phi S^\alpha \zeta^\alpha D_i^\alpha \nabla \widetilde{c}_i^\alpha\Big) = 0,\ i \in \mathcal{C}, \\ \sum_{i\in\mathcal{C}} \widetilde{c}_i^g(f, \widetilde{P}^g, \widetilde{P}^l) = 1, \\ \sum_{i\in\mathcal{C}} \widetilde{c}_i^l(f, \widetilde{P}^g, \widetilde{P}^l) = 1, \end{array}\right. \tag{15}$$

where

$$\left\{\begin{array}{l} \mathbf{V}^\alpha = -\frac{k_r^\alpha(S^\alpha)}{\mu^\alpha} K\Big(\nabla\widetilde{P}^\alpha - \rho^\alpha \mathbf{g}\Big),\ \alpha \in \mathcal{P}, \\ S^g + S^l = 1, \\ S^l = \widetilde{P}_c^{-1}(\widetilde{P}^g - \widetilde{P}^l). \end{array}\right. \tag{16}$$

The same discretization will be used for this formulation as for the previous ones. The two main advantages of this formulation are the absence of inequality constraints to express the phase transitions, and the fix set of unknowns and equations. In addition even the choice of the secondary unknowns can be fixed, choosing two fixed fugacities (for instance f_e and f_{j_1} with the largest Henry constant $H_{j_1}(T)$ provided that the condition $H_{j_1} \neq P_{sat}(T)\exp\Big(\frac{-(P^g-P^l)}{\zeta^l(P^l)RT}\Big)$ is satisfied). This means that a classical Newton Raphson algorithm can be used with also a simplified computation of the Jacobian. On the other hand this formulation also increases the non linearities due to the composition of functions which might increase the stiffness of the non linear systems.

3 Numerical comparison of the three formulations

In this section, the PSC, PSF and PPF formulations are compared in terms of solution and of non linear convergence on 1D and 3D test cases. In all test cases, a sub-relaxation of the Newton type solver is used. The relaxation parameter is computed at each Newton iteration by prescribing a maximum variation of the saturation for the PSF and the PSC formulations while a maximum variation of the capillary pressure is prescribed for the PPF formulation.

Note that the norm of the residual is computed as the sum over all components of the l^1 norm of each component mole balance equation residual. The non linear convergence criteria is prescribed on the relative norm of the residual defined by the ratio of the residual norm by the initial residual norm.

3.1 One dimensional test cases

3.1.1 Drying by suction

This test case proposed by Andra [17] modelizes the drying of geological radioactive waste disposal at the interface between the ventilation gallery and the porous media initially saturated with pure water. We consider an horizontal one dimensional domain $(0, L)$, with $L = 10$ m, representing the storage in the neighbourhood of the gallery located at the right end $x = L$. The temperature is fixed at $T = 300$ K for the sake of simplicity. The rock is considered to be the Callovo-Oxfordian argillites (COx) of homogeneous porosity $\phi = 0.15$ and permeability $K = 5\ 10^{-20}$ m^2. The relative permeabilities of the liquid and gas phases, and the inverse of the capillary pressure are defined by the following Van Genuchten laws

$$k_r^l(S^l) = \begin{cases} 0 & \text{if} \quad S^l < S_{lr}, \\ 1 & \text{if} \quad S^l > 1 - S_{gr}, \\ \sqrt{\bar{S}^l}\Big(1 - (1 - (\bar{S}^l)^{1/m})^m\Big)^2 & \text{if} \quad S_{lr} \leq S^l \leq 1 - S_{gr}, \end{cases} \tag{17}$$

$$k_r^g(S^g) = \begin{cases} 0 & \text{if} \quad S^g < S_{gr}, \\ 1 & \text{if} \quad S^g > 1 - S_{lr}, \\ \sqrt{1 - \bar{S}^l}\Big(1 - (\bar{S}^l)^{1/m}\Big)^{2m} & \text{if} \quad S_{gr} \leq S^g \leq 1 - S_{lr}, \end{cases} \tag{18}$$

and

$$P_c^{-1}(p_c) = S_{lr} + (1 - S_{lr} - S_{gr})\frac{1}{\Big(1 + (\frac{p_c}{P_r})^n\Big)^m}, \tag{19}$$

$$P_c(S^l) = P_r\left(\left(\bar{S}^l\right)^{-\frac{1}{m}} - 1\right)^{\frac{1}{n}}, \tag{20}$$

with

$$\bar{S}^l = \frac{S^l - S_{lr}}{1 - S_{lr} - S_{gr}},$$

and the parameters $n = 1.49$, $m = 1 - \frac{1}{n}$, the residual liquid and gas saturations $S_{lr} = 0.40$, $S_{gr} = 0$, and $P_r = 15\ 10^6$ Pa (see Figure 1).

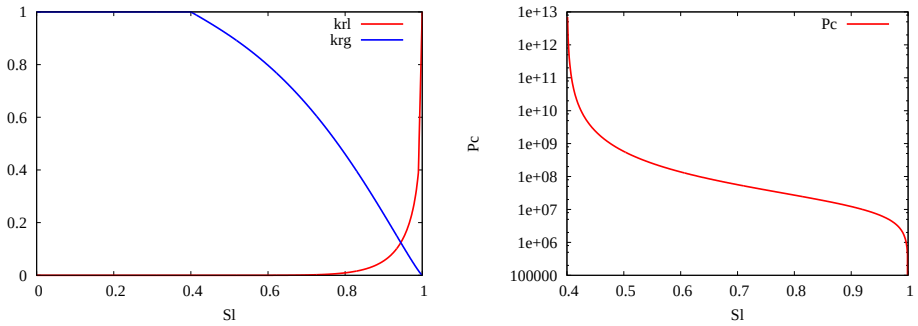

Figure 1: Left: relative permeabilities of the gas and liquid phase k_r^α, $\alpha \in \mathcal{P}$ function of the liquid saturation S^l. Right: capillary pressure P_c (in Pa) function of S^l.

The liquid and gas phases are modelized as mixtures of two components water denoted by e and air denoted by a. Their thermodynamical laws are defined by the constant liquid molar density $\zeta^l = 1000/0.018$ mol.m^{-3}, the perfect gas molar density $\zeta^g = \frac{P^g}{RT}$, with $R = 8.314$ J.K^{-1}.mol^{-1}, and the constant liquid and gas viscosities $\mu^l = 10^{-3}$ Pa.s, and $\mu^g = 18.51\ 10^{-6}$ Pa.s. The vapor pressure is defined by the correlation $P_{sat}(T) = 1.013\ 10^5 e^{13.7-5120/T}$ Pa, and the Henry constant of the air component is set to $H_a = 6.467\ 10^9$ Pa. The Fick diffusion coefficients are fixed to $D_e^g = D_a^g = 10^{-7}$ m^2.s^{-1}, and $D_e^l = D_a^l = 3\ 10^{-9}$ m^2.s^{-1}.

The initial and left end conditions are defined by a liquid phase $S^l = 1$ composed of pure water $c_e^l = 1$, $c_a^l = 0$ at the pressure $P^l = P_0^l = 40\ 10^5$ Pa.

At the interface with the gallery, the gas is defined by its pressure $P^g = P_L^g = 10^5$ Pa, its temperature T, and its relative humidity

$$H_r = \frac{c_e^g P_L^g}{P_{sat}(T)} = 0.5\,.$$

It results that the gas molar composition is given by $c_e^g = \frac{H_r P_{sat}(T)}{P_L^g}$, $c_a^g = 1 - c_e^g$. Assuming that the liquid phase is present at the interface, we deduce from the thermodynamical equilibrium that

$$P_L^l = P_L^g - \zeta^l RT\ \ln(\frac{1 - c_a^g P_L^g / H_a(T)}{H_r})$$

and

$$S_L^l = P_c^{-1}(P_L^g - P_L^l) > S_{lr}.$$

Since the solution exhibits a steep liquid pressure gradient at the right end, the mesh will be locally refined around $x = L$ using the following family of meshes. Let $\Delta x_r < L$, $r > 1$, $\Delta x_l < \Delta x_r < L$ be given parameters for the definition of the mesh. Numbering the cells from right to left, the first cell $[x_1, L]$ is of size $\Delta x_1 = \Delta x_r$, with left end $x_1 = L - \Delta x_1$, and we set for the cell $[x_{i+1}, x_i]$, $\Delta x_{i+1} = r\Delta x_i$,

$x_{i+1} = x_i - \Delta x_{i+1}$. Let N_1 be the last index i such that $\Delta x_i > \Delta x_l$ and $x_i > 0$, we set $N_2 = \left[\frac{x_{N_1}}{\Delta x_l}\right]$, $N = N_1 + N_2$, and $\Delta x_i = \frac{L - x_{N_1}}{N_2}$ for $i = N_1 + 1, \cdots, N$.

In the following numerical experiments we will consider the 5 following meshes

$$\begin{array}{llllll} N = 27 & \text{with} & r = 2, & \Delta x_r = 10^{-3}, & \Delta x_l = 0.5, \\ N = 60 & \text{with} & r = 1.4, & \Delta x_r = 10^{-4}, & \Delta x_l = 0.5/2, \\ N = 126 & \text{with} & r = 1.2, & \Delta x_r = 10^{-5}, & \Delta x_l = 0.5/4, \\ N = 265 & \text{with} & r = 1.1, & \Delta x_r = 10^{-6}, & \Delta x_l = 0.5/8, \\ N = 559 & \text{with} & r = 1.05, & \Delta x_r = 10^{-7}, & \Delta x_l = 0.5/16. \end{array} \tag{21}$$

The simulation is run over the time interval $(0, T)$ with $T = 10$ years, an initial time step of 1 hour, and a maximum time step of 30 days.

Figure 1 exhibits the gas saturation, and the extended gas and liquid pressures $\widetilde{P}^g$, $\widetilde{P}^l$ at different times obtained with the mesh $N = 559$ and the PPF formulation. A zoom at the right end is exhibited in Figure 2 showing the steep gradient of the liquid and gas pressures at a scale of say 0.1 mm which justifies the use of the exponentially refined meshes. Figure 3 exhibits the extended air molar fraction in the gas phase $\widetilde{c}_a^g$ at final time with and without Fickian diffusion for the liquid and gas phases. In view of the position of the gas front at time $t = 10$ years exhibited Figure 1 in blue located at roughly $x = 5.3$ m, and of the position of the air front (pink curve) without diffusion, we clearly deduce that the gas appear by vaporization of the water first. This is confirmed if the diffusion is added in the liquid phase only (blue curve). In that case, the air component diffuses in the liquid phase and the vaporization of the liquid makes it appear in the gas phase. With the diffusion in the gas phase only, the position of the air front (red curve) matches with the position of the gas front showing the dominant diffusion compared with the Darcy convection. The green curve exhibits the case with diffusion in both phases. In that case the air is diffused in the liquid phase and the extended air molar fraction in the gas phase at equilibrium with the liquid phase is non zero.

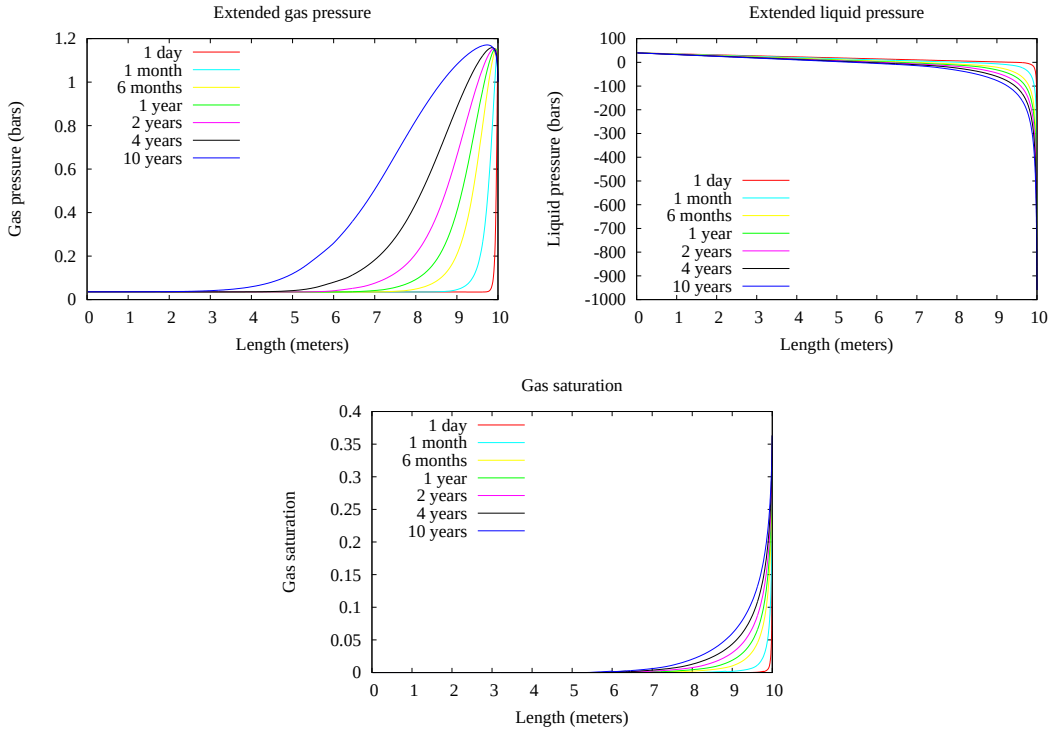

Figure 2: Gas saturation, and extended gas and liquid pressures $\widetilde{P}^g$, $\widetilde{P}^l$ at times $t = 1$ day, 1 month, 6 months, 1 year, 2 years, 4 years, and 10 years obtained with the mesh $N = 559$ and the PPF formulation.

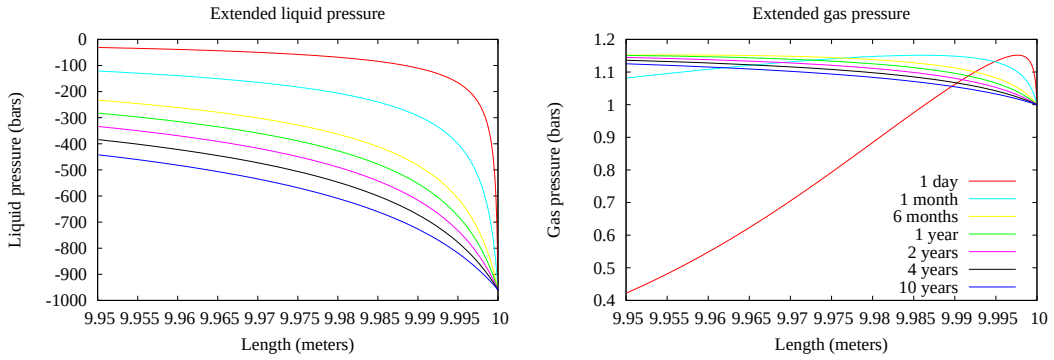

Figure 3: Extended gas and liquid pressures $\widetilde{P}^g$, $\widetilde{P}^l$ at the gallery boundary at times $t = 1$ day, 1 month, 6 months, 1 year, 2 years, 4 years, and 10 years obtained with the mesh $N = 559$ and the PPF formulation.

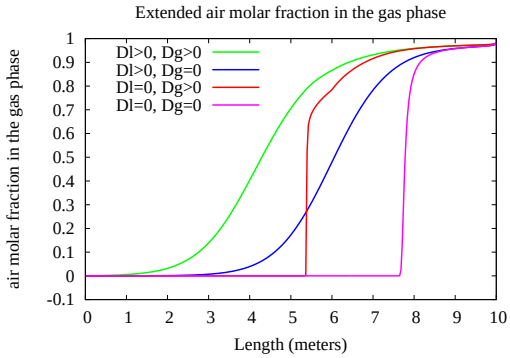

Figure 4: Extended air molar fraction in the gas phase $\widetilde{c}_a^g$ in the four cases (i) $D^l = D^g = 0$ m^2.s^{-1}; (ii) $D^l = 0$ m^2.s^{-1}, $D^g = 10^{-7}$ m^2.s^{-1}; (iii) $D^l = 3\ 10^{-9}$ m^2.s^{-1}, $D^g = 10^{-7}$ m^2.s^{-1}; (iv) $D^l = 3\ 10^{-9}$ m^2.s^{-1}, $D^g = 0$ m^2.s^{-1} at time $t = 10$ years obtained with the mesh $N = 559$ and the PPF formulation.

At the interfaces between two phase and single phase regions, differences could appear especially on coarse meshes between the discrete solutions of the PPF formulation and of the PSC and PSF formulations due to the extension of the pressure $\widetilde{P}^\alpha$ in the absence of the phase α used in the PPF formulation. To check this, the solutions obtained with the three formulations are compared on the coarse mesh $N = 27$ in figure 4. The three solutions are almost the same, and we have checked that the slight differences are due to the regularization of the Van Genuchen capillary pressure for the formulations PSF and PSC to avoid an infinite derivative at $S^l = 1$. This regularization uses a continuous linear extension for $S^l > 1 - \epsilon$ with $\epsilon = 0.005$. It is not required for the PPF formulation since it only uses the inverse of the capillary pressure function.

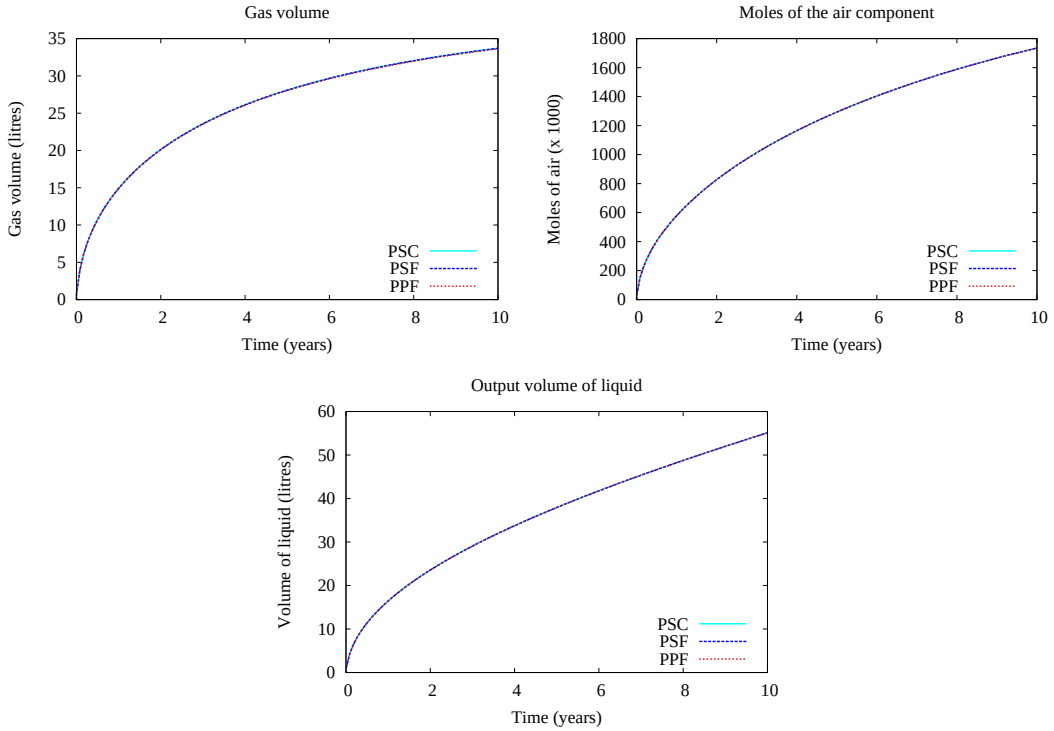

Figure 5: Comparison of the gas volume, the number of moles of the air component, and the output volume of liquid at time $t = 10$ years obtained with the mesh $N = 27$ and the three formulations PPF, PSF and PSC.

Convergence to a stationary analytical solution: a stationary solution can be computed for this test case assuming no dissolution of the gaseous component a, and no Fickian diffusion. This solution is defined by

$$P^l(x) = \begin{cases} P_L^g + \frac{x-x_I}{x_I}(P_L^g - P_0^l), & x \in [0, x_I], \\ P_L^g - \phi^{-1}\left(\frac{x_I-x}{x_I}(P_L^g - P_0^l)\right), & x \in]x_I, L], \end{cases}$$

$$\widetilde{P}^g(x) = \begin{cases} P^l(x) & x \in [0, x_I], \\ P_L^g, & x \in]x_I, L], \end{cases}$$

and $\widetilde{c}_e^g(x) = \frac{P_{sat}(T)}{\widetilde{P}^g(x)} e^{-\frac{\widetilde{P}^g(x) - P^l(x)}{\zeta^l RT}}$, $\widetilde{c}_a^g(x) = 1 - \widetilde{c}_e^g(x)$, where the position of the stationary gas front is given by

$$x_I = \frac{(P_0^l - P_L^g)L}{P_0^l - P_L^g + \phi(P_{c,L})},$$

with $P_{c,L} = -\zeta^l RT \log(H_r)$, and $\phi(u) = \int_0^u k_r^l(\widetilde{P}_c^{-1}(u))du$.

This solution has been used to test the numerical convergence of the discrete solutions obtained by the 3 formulations, and no significant differences have been

observed between the three formulations. Hence the results are exhibited in Figure 6 for the PPF formulation only showing the spatial convergence of the finite volume scheme.

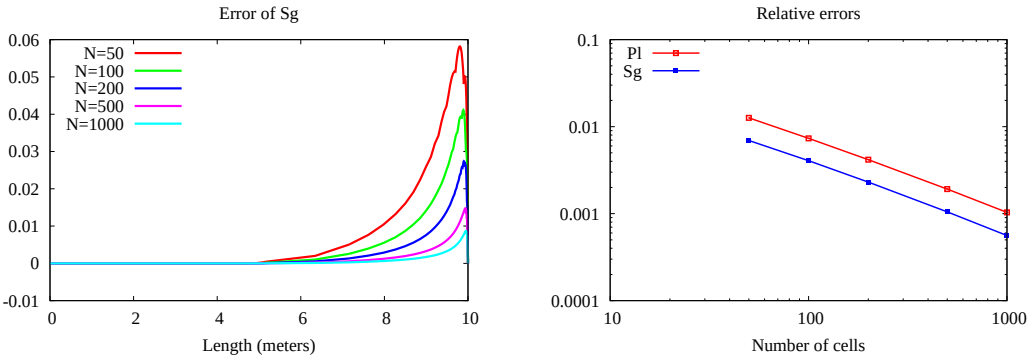

Figure 6: Convergence of the discrete gas saturation S^g and liquid pressure P^l obtained at large times to the stationary analytical solutions for the family of uniform meshes $N = 50, 100, 200, 500, 1000$ and the PPF formulation. The results obtained with the two other formulations are the same.

Comparison of Newton convergence: the three formulations are compared in Figure 1 for all meshes in terms of number of time steps, of time step chops, and total number of Newton iterations. The stopping criteria for the Newton algorithm is chosen as before to be the relative norm of the residual of both mole balance equations to obtain the same criteria for all formulations, and is set to 10^{-7}. Note that a special treatment of the initial guess for the Newton algorithm at initial time had to be used for all formulations in order to obtain the convergence of the first time step. This is due to the incompressibility of the liquid pressure and to the boundary condition at the porous media gallery interface exhibiting a large negative value of the liquid pressure. Basically the initial guess must anticipate the gas appearance at the right boundary.

N	PPF	PSF	PSC
27	132/0/344	132/0/316	132/0/319
60	132/0/355	132/0/329	132/0/335
126	132/0/361	132/0/354	132/0/371
265	132/0/408	132/0/433	132/0/404
559	132/0/435	132/0/496	132/0/567

Table 1: Number of time steps, of time step chops, and total number of Newton iterations for the three formulations PPF, PSF and PSC and for each mesh.

From figure 1, it is clear that the three formulations have roughly the same efficiency in terms of Newton convergence except for the finest mesh for which the PPF formulation is clearly better than the PSC formulation, and slightly better than the PSF formulation. Note that the same behaviour has been observed for increased

time steps, as well as without Fickian diffusion, as well as for modified values of the n parameter of the Van-Genuchten laws.

3.1.2 Drying by gas injection

In order to further compare the three formulations, we consider a test case including gas appearance and liquid disappearance by injection of a dry gas at the right boundary with an imposed gas pressure $P^g = 50\ 10^5$ Pa.

The porous media is the horizontal one dimensional domain $(0, L)$, with $L = 1000$ m of homogeneous porosity $\phi = 0.15$, and permeability $K = 10^{-12}$ m^2. The temperature is fixed to $T = 360$ K.

The relative permeabilities and the capillary pressure are again given by the Van Genuchten laws (17), (18), (19) with parameters $n = 4$, $S_{lr} = 0.4$, $S_{gr} = 0$, and $P_r = 10^5$ Pa. The capillary pressure is extended linearly to $S^l = 0$ between $(S^l, p_c) = (P_c^{-1}(p_{c,0}),\ p_{c,0})$ and $(S^l, p_c) = (0,\ 2\ p_{c,0})$ with $p_{c,0} = 4P_r$ to account for the liquid disappearance.

The liquid and gas phases are still modelized as mixtures of water and air components with the same molar densities, viscosities, and vapor pressure as in the previous test case. The Henry constant for the air component is here fixed to $H_a = 10^8$ Pa, and the Fick diffusion can be neglected compared with the Darcy convection.

The initial and left end conditions are defined by a pure water liquid phase $S^l = 1$ of composition $c_e^l = 1$, $c_a^l = 0$ and pressure $P^l = 40\ 10^5$ Pa. At the right end, the gas phase $S^g = 1$ is injected with the composition $c_e^g = 5\ 10^{-4}$, $c_a^g = 1 - c_e^g$ and the pressure $P^g = 50\ 10^5$ Pa.

The mesh is uniform with the number of cells denoted by N, and the simulation is run over the time interval $(0, T)$ with $T = 40$ years, an initial time step of 1 hour, a maximum time step of 5 days until the gas reaches the left end, and a maximum time step of 1 year in the remaining of the simulation.

Figure 7 exhibits the gas saturation front at different times obtained with the PPF formulation with $N = 100$. The gas hydrodynamic front propagates from right to left at the beginning of the simulation until it reaches the left end, next, the liquid saturation decreases to values close to the residual saturation corresponding to the immobility of the liquid phase, and the liquid begins to disappear at a larger time scale by vaporization of the water and air components in the injected dry gas.

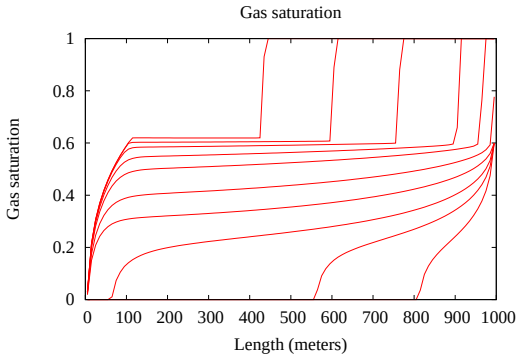

Figure 7: Gas saturation at times $t = 1$, 3, 6 months, and $t = 1$, 2, 5, 10, 20, 30, 40 years obtained with the mesh $N = 100$ and the PPF formulation .

The solutions obtained with the three formulations are as in the previous test case compared on the coarse mesh $N = 20$ in Figure 8 which exhibits no significant differences.

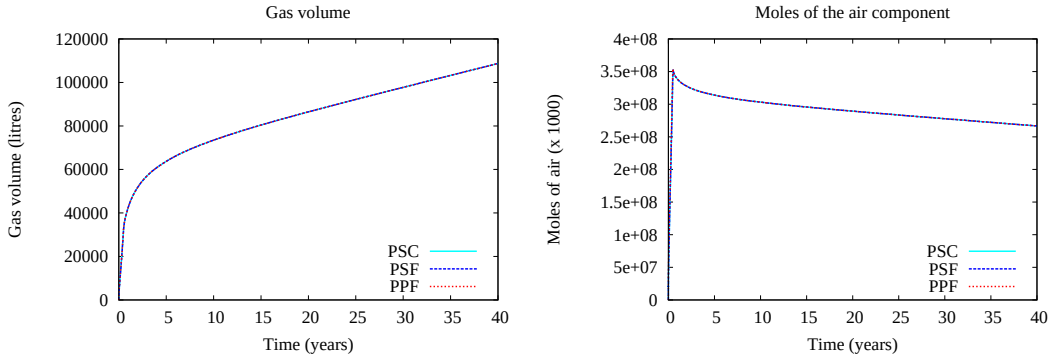

Figure 8: Comparison of the gas volume and the number of moles of the air component as a function of time obtained with the mesh $N = 20$ and the three formulations PPF, PSF and PSC.

Comparison of Newton convergence: We compare as in the previous test case the different formulations in Figure 2. The non linear stopping criteria is the same as in the previous test case. The pressure pressure formulation PPF_2 includes a modification of the Newton algorithm compared with the previous pressure pressure formulation here denoted by PPF_1. This modification forces the Newton iterates to pass by the phase transition points $\widetilde{P}^g - \widetilde{P}^l = P_c(1)$ or $\widetilde{P}^g - \widetilde{P}^l = P_c(0)$ once at each time step and in each cell if a phase transition is observed at this cell at this time step during the Newton algorithm. We observe a considerable improvement of the Newton convergence using this trick although it remains less efficient than the two other formulations.

It seems that the pressure pressure formulation has difficulties in that test case

to deal with the gas phase appearance which was not the case for the previous Andra test case. It may be due to the fact that in the previous test case, the gas front is governed by capillary effects (well approximated by Richards equation), while here it appears by transport of the air component.

N	PPF_1	PPF_2	PSF	PSC
20	192/12/1500	158/0/686	158/0/527	158/0/519
40	224/18/2324	169/1/943	165/0/677	165/0/678
80	272/31/3562	170/1/1192	166/0/900	166/0/900
160	431/74/6702	197/9/2098	166/0/1339	172/2/1477

Table 2: Number of time steps, of time step chops, and total number of Newton iterations for the three formulations PPF, PSF and PSC and for each mesh. The pressure formulation PPF_2 includes a modification of the Newton algorithm compared with the previous PPF_1 pressure pressure formulation.

3.2 Three dimensional test cases

In this section, the Vertex Approximate Gradient (VAG) discretization is introduced for the PPF and PSF formulation of our gas liquid compositional model. The discretization takes into account discontinuous capillary pressures in order to capture the saturation jump at different rocktype interfaces. Then, the PSF and PPF formulations combined with the VAG discretization are compared on two 3D heterogeneous test cases.

In both test cases, we consider the gas liquid thermodynamical model described in section 2 with the three components carbon dioxide (c), air (a) and water (e) with Molar masses $M_c = 44$ g, $M_a = 29$ g, $M_e = 18$ g, a constant temperature $T = 300$ K, the constant liquid molar density $\zeta^l = 1000/0.018$ mol.m^{-3}, the perfect gas molar density $\zeta^g = \frac{P^g}{RT}$, with $R = 8.314$ J.K^{-1}.mol^{-1}, and the constant liquid and gas viscosities $\mu^l = 10^{-3}$ Pa.s, and $\mu^g = 18.51\ 10^{-6}$ Pa.s. The vapor pressure is defined by the correlation $P_{sat}(T) = 1.013\ 10^5 e^{13.7-5120/T}$ Pa, and the Henry constants of the carbon dioxide and air components are set to $H_c(T) = 10^9$ Pa, and $H_a(T) = 6.467\ 10^9$ Pa. No Fickian diffusion is considered.

Note that the PSC formulation is no longer considered in this section since it is very close to the PSF formulation for our gas liquid thermodynamical model as exhibited by the 1D test cases.

3.3 Vertex Approximate Gradient discretization

The Vertex Approximate Gradient (VAG) discretization [10] is a finite volume discretization of diffusion problem adapted to general meshes and heterogenous anisotropic media. It has been extended to multiphase Darcy flows in [11] for compositional models, and to two phase flows with discontinuous capillary pressures in [12] in order to take into account accurately the saturation jump at the interfaces between different rocktypes using a pressure pressure formulation.

Let us consider a polyhedral mesh and denote by $\mathcal{M}$ the set of cells κ, by $\mathcal{V}$ the set of vertices $\mathbf{s}$, by $\mathcal{V}_\kappa$ the set of vertices of each cell $\kappa \in \mathcal{M}$, and by $\mathcal{M}_\mathbf{s}$ the set of cells sharing the node $\mathbf{s}$. Let $X = \mathbb{R}^\mathcal{M} \oplus \mathbb{R}^\mathcal{V}$ denote the vector space of degrees of freedom of the VAG scheme including nodal and cell unknowns. The VAG discretization builds fluxes $F_{\kappa,\mathbf{s}}$ connecting each cell κ to its vertices $\mathbf{s} \in \mathcal{V}_\kappa$ and defined for any $u \in X$ by

$$F_{\kappa,\mathbf{s}}(u) = \sum_{\mathbf{s}' \in \mathcal{V}_\kappa} T_\kappa^{\mathbf{s},\mathbf{s}'}(u_\kappa - u_{\mathbf{s}'}),$$

where $T_\kappa = (T_\kappa^{\mathbf{s},\mathbf{s}'})_{\mathbf{s},\mathbf{s}' \in \mathcal{V}_\kappa}$ is a positive definite matrix depending on the geometry of the cell κ and on the permeability tensor K_κ assumed to be constant in each cell κ.

The control volumes of the VAG discretization on which the mole balance of each component is written, are defined at each cell $\kappa \in \mathcal{M}$ and at each node $\mathbf{s} \in \mathcal{V} \setminus \mathcal{V}_D$ excluding the nodes with Dirichlet boundary conditions $\mathcal{V}_D$. The VAG discretization does not use the geometry of these control volumes but only needs to define the fractions $\alpha_{\kappa,\mathbf{s}} \geq 0$ distributing the volume of each cell $\kappa \in \mathcal{M}$ to its nodes $\mathbf{s} \in \mathcal{V}_\kappa \setminus \mathcal{V}_D$, constrained to satisfy the condition $1 - \sum_{\mathbf{s} \in \mathcal{V}_\kappa \setminus \mathcal{V}_D} \alpha_{\kappa,\mathbf{s}} \geq 0$. In practice, the choice of the fractions $\alpha_{\kappa,\mathbf{s}}$ is done in order to avoid the mixing of different rocktypes at nodal control volumes. This choice of the control volumes improves the discretization of heterogeneous test cases compared with usual Control Volume Finite Element (CVFE) approaches.

Let U denote the unknowns of the compositional model with $U = \left(P^g, P^l, f\right)$ for the PPF formulation (dropping the tilde for conveniency), and $U = \left(P^g, P^l, S^g, S^l, f\right)$ for the PSF formulation. Let us denote by U_κ the cell unknowns, by $U_\mathbf{s}$ the node unknowns, and let us set $U_{\nu_\kappa} = \left(U_\mathbf{s}\right)_{\mathbf{s} \in \mathcal{V}_\kappa}$. For conveniency in the notations, the physical laws in both formulations will be considered as fonctions of U and denoted by $c_i^\alpha(U)$ (dropping the tilde), $\rho^\alpha(U)$, $\zeta^\alpha(U)$, and $\mu^\alpha(U)$.

The VAG discretization of two phase Darcy flows can be adapted to take into account the jump of the saturations at different rocktype interfaces. The capillary pressures and relative permeabilities are assumed to be cellwise constant and denoted by $P_{c,\kappa}$, $k_{r,\kappa}^\alpha$ for all $\kappa \in \mathcal{M}$. The PPF formulation has the advantage to work directly with phase pressures as primary unknowns which can be considered continuous at different rocktype interfaces. Then, following [12], it naturally leads to define the discrete saturations as follows:

$$S_\kappa^l = \widetilde{P}_{c,\kappa}^{-1}(P_\kappa^g - P_\kappa^l), \quad S_\kappa^g = 1 - S_\kappa^l \text{ for all } \kappa \in \mathcal{M},$$
$$S_{\kappa,\mathbf{s}}^l = \widetilde{P}_{c,\kappa}^{-1}(P_\mathbf{s}^g - P_\mathbf{s}^l), \quad S_{\kappa,\mathbf{s}}^g = 1 - S_{\kappa,\mathbf{s}}^l \text{ for all } \mathbf{s} \in \mathcal{V}_\kappa, \kappa \in \mathcal{M}.$$

In the case of the PSF formulation, the saturations S_κ^α and $S_\mathbf{s}^\alpha$, $\alpha = g, l$, are primary unknowns and one capillary pressure $P_{c,\mathbf{s}}$ must be prescribed at each node $\mathbf{s} \in \mathcal{V}$. If $P_c(S^l = 1) = 0$ for all rocktypes (no entry pressure), all rocktypes among those in the cells $\kappa \in \mathcal{M}_\mathbf{s}$ can be chosen, otherwise, one must choose one rocktype with the

lowest entry pressure. Then, in order to account for the saturation jump at different rocktype interfaces, the discretization uses the following saturations at the interfaces

$$S^l_{\kappa,\mathbf{s}} = \widetilde{P}^{-1}_{c,\kappa}\Big(P_{c,\mathbf{s}}(S^l_{\mathbf{s}})\Big), \quad S^g_{\kappa,\mathbf{s}} = 1 - S^l_{\kappa,\mathbf{s}} \text{ for all } \mathbf{s} \in \mathcal{V}_\kappa, \kappa \in \mathcal{M}.$$

The discretization of the Darcy fluxes combines the VAG fluxes, the above definition of the saturations, and a phase by phase upwinding of the mobility terms w.r.t. the sign of the flux:

$$V^\alpha_{\kappa,\mathbf{s},i}(U_\kappa, U_{\nu_\kappa}) = \Big(\frac{\zeta^\alpha c^\alpha_i}{\mu^\alpha}\Big)(U^\alpha_{\kappa,\mathbf{s}})k^\alpha_{r,\kappa}(S^\alpha_{\kappa,\mathbf{s},up})\Big(F_{\kappa,\mathbf{s}}(P^\alpha) + g\rho^\alpha_{\kappa,\mathbf{s}}F_{\kappa,\mathbf{s}}(Z)\Big),$$

with the upwindings

$$U^\alpha_{\kappa,\mathbf{s}} = \begin{cases} U_\kappa & \text{if} \quad F_{\kappa,\mathbf{s}}(P^\alpha) + g\rho^\alpha_{\kappa,\mathbf{s}}F_{\kappa,\mathbf{s}}(Z) \geq 0, \\ U_{\mathbf{s}} & \text{else}, \end{cases}$$

$$S^\alpha_{\kappa,\mathbf{s},up} = \begin{cases} S^\alpha_\kappa & \text{if} \quad F_{\kappa,\mathbf{s}}(P^\alpha) + g\rho^\alpha_{\kappa,\mathbf{s}}F_{\kappa,\mathbf{s}}(Z) \geq 0, \\ S^\alpha_{\kappa,\mathbf{s}} & \text{else}, \end{cases}$$

with the average density $\rho^\alpha_{\kappa,\mathbf{s}} = \frac{\rho^\alpha(U_\kappa)+\rho^\alpha(U_{\mathbf{s}})}{2}$, the vector of the vertical coordinates at all d.o.f. $Z = \Big(z_\kappa, \kappa \in \mathcal{M}, z_{\mathbf{s}}, \mathbf{s} \in \mathcal{V}\Big)$, and the discrete phase pressure at all d.o.f. $P^\alpha = \Big(P^\alpha_\kappa, \kappa \in \mathcal{M}, P^\alpha_{\mathbf{s}}, \mathbf{s} \in \mathcal{V}\Big)$.

With these notations, the discrete mole balance of each component $i \in \mathcal{C}$ in each control volume writes for both formulations: given $U^0 = (U^0_\nu)_{\nu\in\mathcal{M}\cup\mathcal{V}}$ at initial time, find $U^n = (U^n_\nu)_{\nu\in\mathcal{M}\cup\mathcal{V}}$ for all times t^n, $n = 1, \cdots, N$ such that

$$\begin{cases} (1 - \sum_{\mathbf{s}\in\mathcal{V}_\kappa\setminus\mathcal{V}_D} \alpha_{\kappa,\mathbf{s}})\phi_\kappa \dfrac{n_{i,\kappa}(U^n_\kappa) - n_{i,\kappa}(U^{n-1}_\kappa)}{t^n - t^{n-1}} + \sum_{\alpha\in\mathcal{P}}\sum_{\mathbf{s}\in\mathcal{V}_\kappa} V^\alpha_{\kappa,\mathbf{s},i}(U^n_\kappa, U^n_{\nu_\kappa}) = 0, \ \kappa \in \mathcal{M}, \\ \sum_{\kappa\in\mathcal{M}_{\mathbf{s}}} \alpha_{\kappa,\mathbf{s}}\phi_\kappa \dfrac{n_{i,\kappa,\mathbf{s}}(U^n_{\mathbf{s}}) - n_{i,\kappa,\mathbf{s}}(U^{n-1}_{\mathbf{s}})}{t^n - t^{n-1}} - \sum_{\alpha\in\mathcal{P}}\sum_{\kappa\in\mathcal{M}_{\mathbf{s}}} V^\alpha_{\kappa,\mathbf{s},i}(U^n_\kappa, U^n_{\nu_\kappa}) = 0, \ \mathbf{s} \in \mathcal{V}\setminus\mathcal{V}_D, \end{cases}$$

with

$$n_{i,\kappa}(U_\kappa) = \sum_{\alpha\in\mathcal{P}} \zeta^\alpha(U_\kappa)S^\alpha_\kappa c^\alpha_i(U_\kappa), \ n_{i,\kappa,\mathbf{s}}(U_{\mathbf{s}}) = \sum_{\alpha\in\mathcal{P}} \zeta^\alpha(U_{\mathbf{s}})S^\alpha_{\kappa,\mathbf{s}} c^\alpha_i(U_{\mathbf{s}}),$$

$\phi_\kappa = \int_\kappa \phi(\mathbf{x})d\mathbf{x}$, and specified Dirichlet boundary conditions $U^n_{\mathbf{s}}$ for all $\mathbf{s} \in \mathcal{V}_D$. The mole balance equations are completed by the following local closure laws in each control volume $\nu \in \mathcal{M}\cup\mathcal{V}\setminus\mathcal{V}_D$ which write

$$\begin{cases} S^{g,n}_\nu + S^{l,n}_\nu = 1, \\ P^{g,n}_\nu - P^{l,n}_\nu = P_{c,\nu}(S^{l,n}_\nu), \\ S^{\alpha,n}_\nu\Big(\sum_{i\in\mathcal{C}} c^\alpha_i(U^n_\nu) - 1\Big) = 0, \alpha \in \mathcal{P}, \\ S^{\alpha,n}_\nu \geq 0, \ \sum_{i\in\mathcal{C}} c^\alpha_i(U^n_\nu) \leq 1, \alpha \in \mathcal{P}, \end{cases}$$

for the PSF formulation, and

$$\sum_{i\in\mathcal{C}} c_i^\alpha(U_\nu^n) = 1, \alpha \in \mathcal{P},$$

for the PPF formulation.

The non linear system is solved at each time step using a Newton Raphson algorithm. For the PSF formulation, a Newton-Min algorithm adapted to complementary constraints is used [4]. For the PPF formulation, a usual Newton algorithm is used combined with the same trick as in the 1D drying by gas injection test case forcing the Newton iterates to pass through the phase transition points. In both cases, the Jacobian system is reduced to its Schur complement by elimination of the local closure laws which involves the choice of secondary unknowns among U. This choice depends on the present phases in the case of the PSF formulation and is fixed to two fugacities in the case of the PPF algorithm.

Then, the cell unknowns are eliminated of the linear system without any fill-in using the cell equations and reducing the linear system to the nodal unknowns only.

3.4 Drying by suction

The 1D test case is extended to a 3D geometry using a radial mesh of the domain $(0, L) \times (r_G, r_e) \times (0, 2\pi)$ in cylindrical coordinates with $r_G = 2$ m and $r_e = 10$ m, $L = 100$ m. The mesh is exponentially refined at the boundary of the gallery $r = r_G$ to account for the steep gradient of the capillary pressure at the interface. We consider two rocktypes, corresponding to the Excavation Damaged Zone (EDZ) of COx for $r < 3$ m, and to the COx shale for $r > 3$ m (see Figure 9). The relative permeabilities and capillary pressures are given by the Van-Genuchten laws (17), (18), (19), with the parameters $n = 1.49$, $S_{lr} = 0.4$, $S_{gr} = 0$, $P_r = 15\ 10^6$ Pa for COx, and $n = 1.54$, $S_{lr} = 0.01$, $S_{gr} = 0$, $P_r = 2\ 10^6$ Pa for EDZ. The porosities are constant for each rocktype and equal to $\phi = 0.15$ for COx, and $\phi = 0.3$ for EDZ. The absolute permeability tensor is heterogeneous and anisotropic with $K = \begin{pmatrix} \lambda & 0 & 0 \\ 0 & \lambda & 0 \\ 0 & 0 & \frac{\lambda}{100} \end{pmatrix}$, in the x, y, z Cartesian coordinates where z is the vertical coordinate and x the direction of the Gallery, $\lambda = 5\ 10^{-20}$ m^2 for COx and $\lambda = 10^{-18}$ m^2 for EDZ. Note that the principal directions of K are not aligned with the radial mesh excluding the use of a Two Point Flux Approximation for this test case.

The initial and external boundary ($r = r_e$) conditions are defined by a liquid phase $S^l = 1$ composed of pure water $c_e^l = 1$, $c_a^l = 0$, $c_c^l = 0$ at the hydrostatic pressure $P^l = P_0^l - \rho^l g z$ with $P_0^l = 40\ 10^5$ Pa. At the interface with the gallery, the gas is defined by its constant pressure $P^g = 10^5$ Pa, and its relative humidity function of x along the gallery

$$H_r(x) = \frac{c_e^g P^g}{P_{sat}(T)} = 0.3 + \frac{x}{2L}.$$

The gas molar composition is given by $c_e^g(x) = \frac{H_r(x)P_{sat}(T)}{P^g}$, $c_a^g(x) = c_c^g(x) = \frac{1-c_e^g(x)}{2}$.

We deduce from the thermodynamical equilibrium that

$$P^l(x) = P^g - \zeta^l RT \ln(\frac{1 - c_a^g(x)P^g/H_a(T) - c_c^g(x)P^g/H_c(T)}{H_r(x)}),$$

and

$$S^l(x) = P_c^{-1}(P^g - P^l(x)) > S_{lr}.$$

This variation of the relative humidity along the gallery mimics the coupling of the flow in the gallery with the Darcy flow in the surrounding porous media.

The simulation is run over a period of 20 years with an initial time step of 1000 s and a maximum time step of 30 days on the meshes $n_x \times n_r \times n_\theta$ with $n_x = n_r = n_\theta = n$ and $n = 20, 30, 40, 50, 60$. The linear systems are solved using a GMRes iterative solver preconditioned by an ILU0 preconditioner with the stopping criteria 10^{-6} on the relative residual. The Newton stopping criteria is fixed to 10^{-6} on the relative residual.

Figure 11 exhibits the convergence of the volume of gas and of the liquid volumic outflow in the gallery as a function of time for the family of meshes. The curves are plotted for the PPF formulation only since no visible difference is observed between both formulations. Figure 10 exhibits a transversal cut of the final solutions S^g and $S^g c_e^g$ for both formulations and for the mesh $n = 60$, showing only slight differences in the shape of the fronts between both formulations.

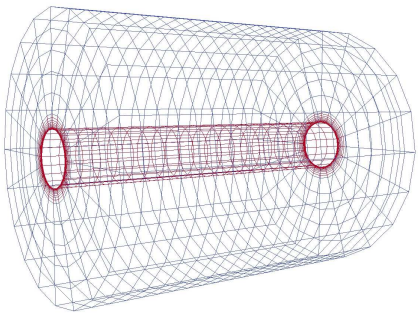

Figure 9: Radial mesh for $n = 20$ with the EDZ rocktype in red.

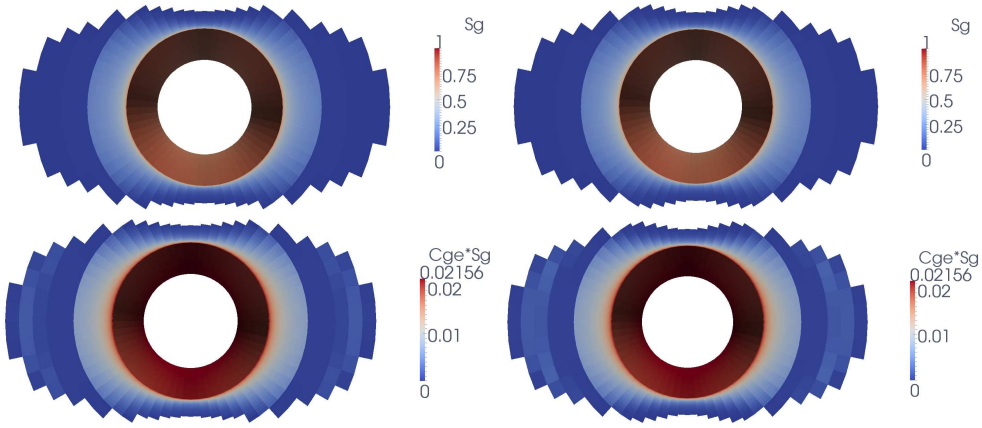

Figure 10: Transversal cut of S^g and of $S^g c_e^g$ at final time obtained on the mesh $n = 60$ for the PPF formulation (left) and the PSF formulation (right).

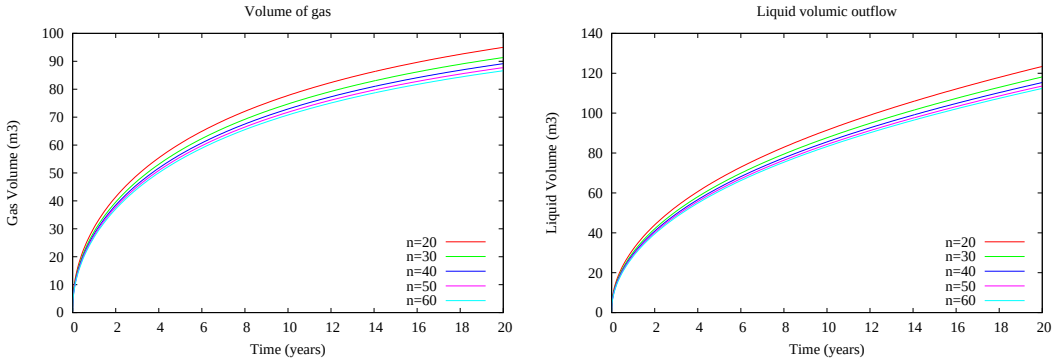

Figure 11: For each mesh $n = 20, 30, 40, 50, 60$: volume of gas in the porous media as a function of time, and volumic cumulative outflow of liquid in the gallery function of time.

Table 3 exhibits the numerical behavior of the simulations for each mesh and for both the PPF and PSF formulations. It is clear that both formulations are very robust for this test case in terms of Newton convergence with an advantage to the PPF formulation for the finest meshes which confirms the results obtained in 1D.

formulation	mesh	$N_{\Delta t}$	N_{Chop}	N_{Newton}	N_{GMRes}	CPU(s)
PPF	$n = 20$	279	0	2.36	16.3	644
PPF	$n = 30$	279	0	2.38	23.5	2527
PPF	$n = 40$	279	0	2.41	31.4	6850
PPF	$n = 50$	279	0	2.42	41.1	14311
PPF	$n = 60$	279	0	2.47	58.3	29338
PSF	$n = 20$	279	0	2.33	16.0	690
PSF	$n = 30$	279	0	2.48	21.9	2807
PSF	$n = 40$	279	0	2.57	29.3	7493
PSF	$n = 50$	279	0	2.7	40.9	21304
PSF	$n = 60$	279	0	2.87	79.7	46985

Table 3: For each mesh and both formulations PPF and PSF: number $N_{\Delta t}$ of successful time steps, number N_{Chop} of time step chops, number N_{Newton} of Newton iterations per successful time step, number N_{GMRes} of GMRes iterations by Newton iteration, CPU time in seconds.

3.5 Migration of gas in a basin with capillary barriers

The second test case is designed to assess the numerical behavior of the two formulations PPF and PSF with discontinuous capillary pressures. We consider the migration of gas in a basin $(0, L) \times (0, L) \times (0, H)$ with $L = H = 100$ m, including two capillary barriers. We consider a 2D geometry exhibited in Figure 14 which can be discretized using a 2D mesh (3D mesh with only one cell in the y direction), and a 3D geometry exhibited in Figure 17 discretized using a 3D mesh. In both figures the barriers are exhibited in red and immersed in a blue drain. The permeabilities are isotropic and equal to $K = 10^{-12}$ m^2 in the drain and to $K = 10^{-14}$ m^2 in the barriers. The porosity is set to $\phi = 0.1$ on the whole basin.

The initial and top boundary ($z = H$) conditions are defined by a liquid phase $S^l = 1$ composed of pure water $c_e^l = 1$, $c_a^l = 0$, $c_c^l = 0$ at the hydrostatic pressure $P^l = P_0^l - \rho^l g z$ with $P_0^l = 15\ 10^5$ Pa. At the bottom boundary $z = 0$, $x^2 + y^2 \leq 25^2$, the gas is injected at the constant pressure $P^g = 16\ 10^5$ Pa, and with the relative humidity

$$H_r = \frac{c_e^g P^g}{P_{sat}(T)} = 0.5.$$

The injected gas molar composition is given by $c_e^g = \frac{H_r P_{sat}(T)}{P^g}$, $c_a^g = c_c^g = \frac{1-c_e^g}{2}$, and the saturation is fixed to $S^g = 0.8$. All the remaining boundaries are impervious.

The capillary pressures exhibited in Figure 12 are given by the Corey laws

$$P_c(S^l) = -10^4 \log(S^l),$$

in the drain, and by

$$P_c(S^l) = \begin{cases} \frac{1-S^l}{1-S_1^l} P_{c,1} & \text{if } S^l > S_1^l, \\ 4\ 10^5 - 10^5 \log(S^l) & \text{if } S^l \leq S_1^l, \end{cases}$$

in the barrier with $P_{c,1} = 4.025\ 10^5$ Pa and $S_1^l = e^{-0.025}$. The entry capillary pressure $p_c = 4\ 10^5$ Pa is chosen to be larger than the gravity load below the first barrier but lower than the gravity load below the second barrier. The relative permeabilities are given by the Corey laws

$$k_r^\alpha(S^\alpha) = (S^\alpha)^2,\ \alpha = g, l,$$

with zero residual saturations.

In view of Figure 13, the reference rocktype for the PSF formulation is chosen to be the barrier rocktype. The reverse choice leads to round off errors in the simulation leading to a wrong solution (at infinite accuracy, both choices should be equivalent since $P_c(S^l = 1) = 0$ for both rocktypes in this test case).

The simulation is run over a period of 40 days with an initial time step of 0.02 days and a maximum time step of 0.1 days on a family of topologically Cartesian meshes of sizes $n \times 1 \times n$ for the 2D geometry (see Figure 14), with $n = 16, 32, 64, 128$, and of sizes for the 3D geometry (see Figure 17) with $n = 16, 32, 48$. The linear solver and the non linear and linear stopping criteria are the same than in the previous test case. If the Newton non linear solver does not converge after 25 iterations, the time step is choped by a factor 2, while the time step is increased of a factor 1.2 after a converged time step until it reaches the maximum time step.

Figure 15 (resp. 18) shows the gas saturation S^g at final time obtained by the PPF and PSF formulations on the different meshes for the 2D (resp. 3D) basin. Figure 16 (resp. 19) shows the volume of air dissolved in the liquid phase function of time for both formulations and for the different meshes of the 2D (resp. 3D) basin. The equivalence between both formulations does not hold at the discrete level due to discrete interfaces between single and two phase regions. Indeed, the extension of the pressure of an absent phase depending on the formulation, the fluxes at such interfaces can also depend on the formulation if the upwinding is on the present phase side. One can only expect that the solutions obtained with both formulations will converge to the same solution when the mesh is refined. This convergence can be observed in Figures 15, 18, 16, 19 especially on the 2D basin using meshes up to $n = 128$. On the 3D basin, we have not been able to refine the mesh further than $n = 48$ due to too large CPU time with the PPF formulation. Nevertheless, the convergence seems also in good way for the 3D basin.

Tables 4 and 5 exhibit the numerical behavior of both formulations showing the good behavior of the PSF formulation while the PPF formulation requires much smaller time steps to solve the non linear systems especially when the mesh is refined. This has been obtained with the improvement of the Newton algorithm imposing the Newton iterates to pass though the phase transition points of the graph $\widetilde{P}_c^{-1}$. Without this modification, the simulation ends before final time with a time step lower than the minimum time step fixed to 10^{-4} days even on the coarsest meshes.

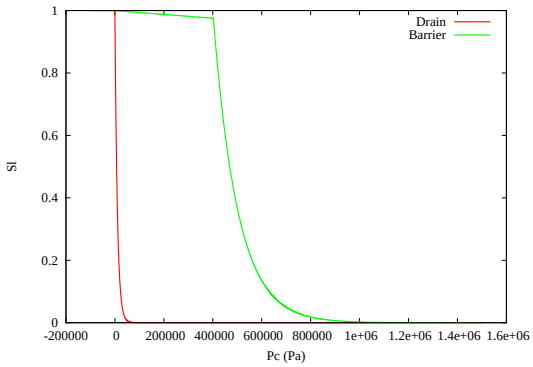

Figure 12: Inverses of the monotone graphs of the capillary pressure in the barrier and in the drain.

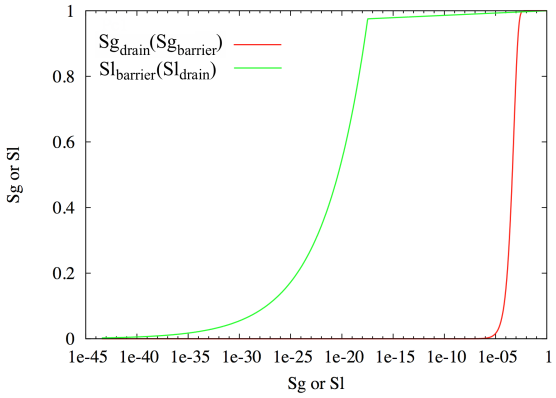

Figure 13: $S^g_{drain} = 1 - P^{-1}_{c,drain}(P_{c,barrier}(1 - S^g_{barrier}))$ function of $S^g_{barrier}$ and $S^l_{barrier} = P^{-1}_{c,barrier}(P_{c,drain}(S^l_{drain}))$ function of S^l_{drain}.

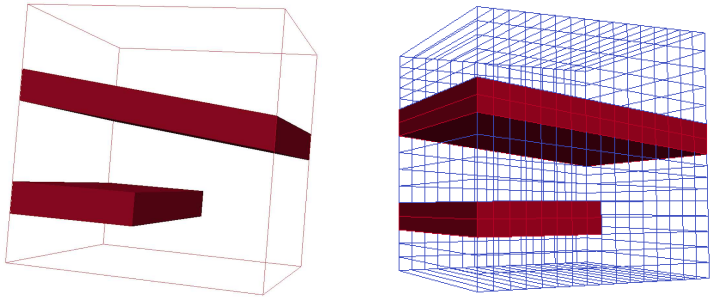

Figure 14: 2D geometry of the Basin domain with the two barriers in red and the surrounding drain. Mesh $16 \times 1 \times 16$ of the basin.

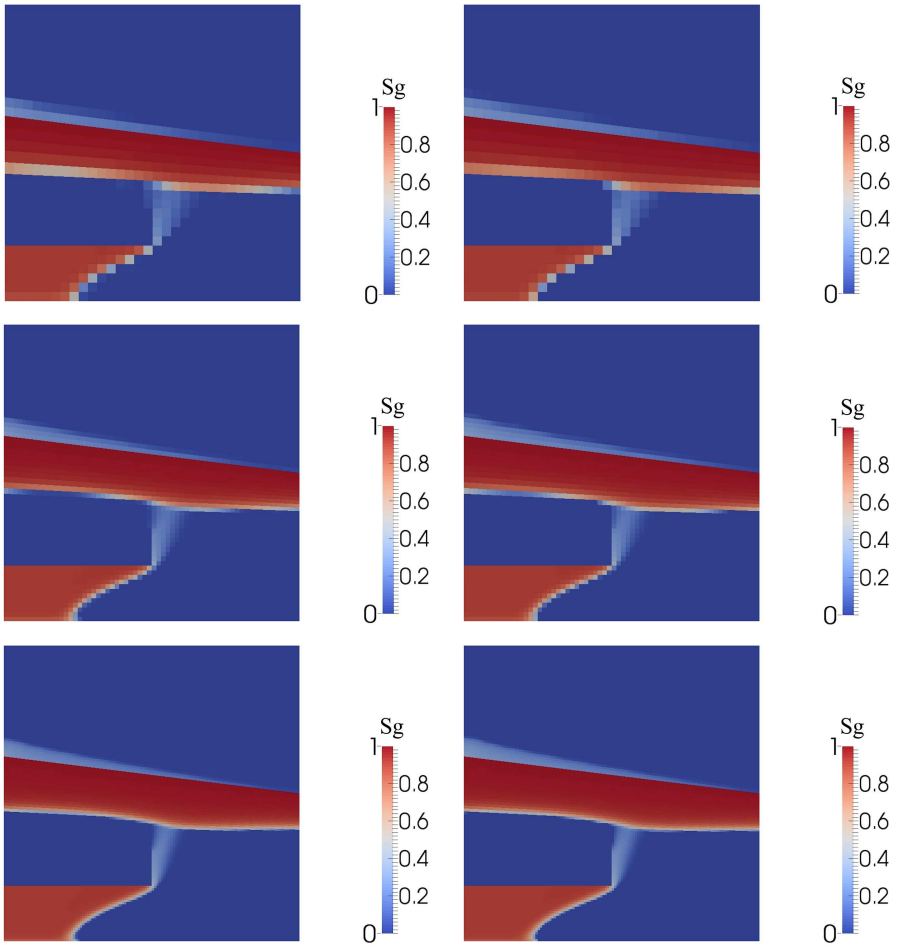

Figure 15: Gas saturation S^g above the threshold 10^{-6} at final time for the PPF (left) and PSF (right) formulations on the meshs $32\times1\times32$, $64\times1\times64$, $128\times1\times128$ of the 2D basin.

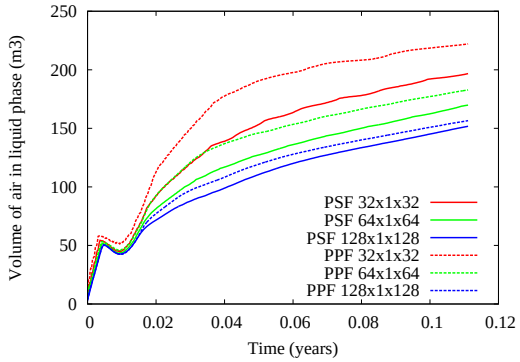

Figure 16: Volume of air dissolved in the liquid phase in the 2D basin function of time for both formulations PSF and PPF and for the family of meshes.

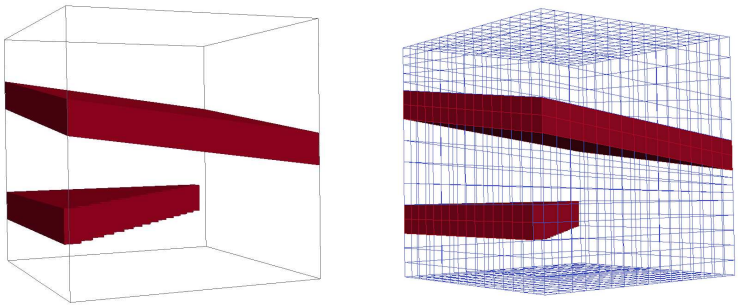

Figure 17: 3D geometry of the Basin domain with the two barriers in red and the surrounding drain. Mesh $16 \times 16 \times 16$ of the basin.

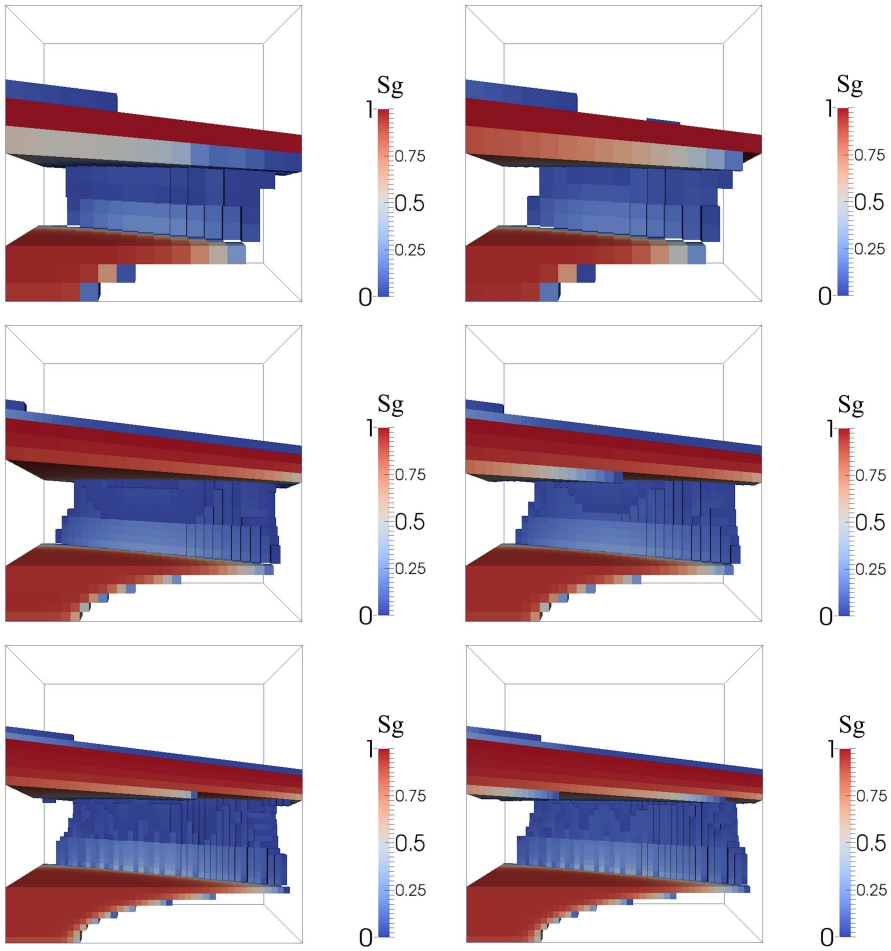

Figure 18: Gas saturation S^g above the threshold 10^{-6} at final time for the PPF (left) and PSF (right) formulations on the meshs $16\times16\times16$, $32\times32\times32$, $48\times48\times48$ of the 3D basin.

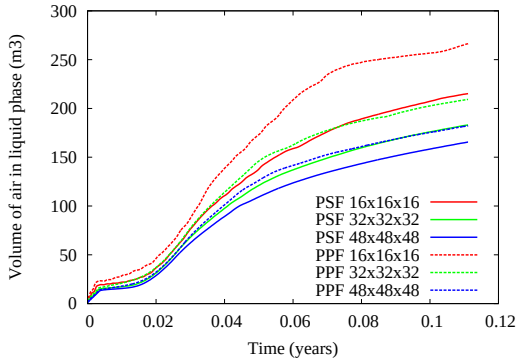

Figure 19: Volume of air dissolved in the liquid phase in the 3D basin function of time for both formulations PSF and PPF and for the family of meshes.

formulation	mesh	$N_{\Delta t}$	N_{Chop}	N_{Newton}	N_{GMRes}	CPU(s)
PSF	$n = 16$	405	0	2.92	13.4	35
PSF	$n = 32$	405	0	3.77	21.6	217
PSF	$n = 64$	405	0	4.75	37.6	1480
PSF	$n = 128$	409	3	6.28	66.7	11820
PPF	$n = 16$	405	0	3.93	13.5	46
PPF	$n = 32$	408	2	7.70	20.0	421
PPF	$n = 64$	525	61	17.65	31.2	6252
PPF	$n = 128$	1175	297	23.78	49.4	98549

Table 4: For each mesh $n \times 1 \times n$ of the 2D basin and both formulations PPF and PSF: number $N_{\Delta t}$ of successful time steps, number N_{Chop} of time step chops, number N_{Newton} of Newton iterations per successful time step, number N_{GMRes} of GMRes iterations by Newton iteration, CPU time in seconds.

formulation	mesh	$N_{\Delta t}$	N_{Chop}	N_{Newton}	N_{GMRes}	CPU(s)
PSF	$n = 16$	405	0	3.87	24.8	781
PSF	$n = 32$	405	0	4.72	48.7	10296
PSF	$n = 48$	407	1	5.34	74.7	49170
PPF	$n = 16$	407	1	5.96	24.7	1146
PPF	$n = 32$	717	151	15.3	43.4	54205
PPF	$n = 48$	1803	472	16.1	56.5	543706

Table 5: For each mesh $n \times n \times n$ of the 3D basin and both formulations PPF and PSF: number $N_{\Delta t}$ of successful time steps, number N_{Chop} of time step chops, number N_{Newton} of Newton iterations per successful time step, number N_{GMRes} of GMRes iterations by Newton iteration, CPU time in seconds.

4 Conclusion

In this paper three formulations of compositional gas liquid two phase flows with phase transitions have been shown to lead to equivalent definitions of the phase transitions. They have been compared in terms of non linear solver convergence and solutions on different 1D and 3D test cases involving gas appearance and liquid disappearance. The VAG discretization has been used in 3D taking into account discontinuous capillary pressures to capture accurately the saturation jump at different rocktype interfaces.

On the drying by suction 1D and 3D test cases, the three formulations lead to quite similar results with a better behavior of the PPF formulation on the finest meshes. On the other hand the PPF formulation has severe difficulties to deal with the gas phase appearance and liquid disappearance in the gas injection test cases, both in 1D and 3D. This difficulty is due to the degeneracy of the inverse of the capillary function $\widetilde{P}_c^{-1}$ at the phase transition points $S^l = 1$ and $S^l = 0$. The Newton convergence has been improved by forcing the Newton iterates to pass through these phase transition points, nevertheless it has not been sufficient to obtain large enough time steps on the gas injection test cases especially when the mesh is refined. This drastic difference of behaviour of the PPF formulation between the two test cases is probably due to the fact that the gas front is dominated by the capillary effect and well approximated by the Richards equation for the drying by suction test case, while it is more dominated by the Buckley Leverett equation and the gravity or pressure gradient terms for the gas injection test cases.

All together, the PSF and PSC formulations clearly outperform the PPF formulation for compositional gas liquid Darcy flows on our set of numerical experiments.

References

[1] K. Aziz, A. Settari, Petroleum Reservoir Simulation. Applied Science Publishers (1979).

[2] O. Angelini, C. Chavant, E. Chénier, R. Eymard, S. Granet, Finite volume approximation of a diffusion-dissolution model and application to nuclear waste storage. Mathematics and Computers in Simulation, 81 (10), pp. 2001-2017, 2011.

[3] Abadpour, A. and Panfilov, M.: Method of negative saturations for modelling two phase compositional flows with oversaturated zones. Transport in porous media, 79,2, pp. 197-214, 2010.

[4] I. Ben Gharbia, J. Jaffré, Gas phase appearance and disappearance as a problem with complementarity constraints, INRIA report, http://hal.inria.fr/hal-00641621, 2011.

[5] A. Bourgeat, M. Jurak, F. Smai, Two phase partially miscible flow and transport in porous media; application to gas migration in nuclear waste repository. Computational Geosciences, 13,1, pp. 29-42, 2009.

[6] K.H. Coats, An equation of state compositional model. SPE Reservoir Simulation Symposium Journal, pp. 363-376, 1980.

[7] K. H. Coats, Implicit compositional simulation of single-porosity and dual-porosity reservoirs. SPE Symposium on Reservoir Simulation, 1989.

[8] H. Cao, Development of techniques for general purpose simulators, PhD, University of Stanfords, 2002.

[9] Jean François Daïan, Equilibre et transfert en milieux poreux, http://hal.inria.fr/docs/00/96/75/30/PDF/ETMP314.pdf

[10] R. Eymard, C. Guichard, and R. Herbin, Small-stencil 3D schemes for diffusive flows in porous media. ESAIM: Mathematical Modelling and Numerical Analysis, 46, pp. 265-290, 2010.

[11] R. Eymard, R. Herbin, C. Guichard, R. Masson, Vertex Centred discretization of compositional Multiphase Darcy flows on general meshes. Comp. Geosciences, vol. 16, issue 4, pp. 987-1005, 2012.

[12] R. Eymard, C. Guichard, R. Herbin, R. Masson, Gradient schemes for two-phase flow in heterogeneous porous media and Richards equation, Journal of Applied Mathematics and Mechanics, published online in august 2013.

[13] R. Huber and R. Helmig, Node-centered finite volume discretizations for the numerical simulation of multi-phase flow in heterogeneous porous media, Computational Geosciences, 4, pp. 141-164, 2000.

[14] A. Lauser, C. Hager, R. Helmig, B. Wohlmuth, A new approach for phase transitions in miscible multi-phase flow in porous media, Advances in Water Resources 34, pp. 957-966, 2011.

[15] S. Kräutle: The semi-smooth Newton method for multicomponent reactive transport with min- erals. Adv. Water Res. 34 (2011), 137-151,

[16] Whitson, C. H. and Michelsen, M. L.: The negative flash. Fluid Phase Equilibria, 53, pp. 51-71, 1989.

[17] MoMaS COUPLEX Workshop, July 26-27 2001, CIRM Luminy-Marseille (France), http://www.ljll.math.upmc.fr/cances/gdrmomas/Exqualif/Couplex/couplex Cemracs2001.html